cells was evaluated by detecting BCECF-AM-positive cells among donor lymphocytes that colonized the spleen, lymph nodes, and peripheral blood.

Statistical analyses

Values of p for differences between groups were determined by Student's t test using Microsoft Excel software. Statistical analyses of measured serum Ig level were performed by Mann-Whitney U test.

Results

Generation of Cas-L-deficient mice

To generate Cas-L-deficient mice, the 1.2-kb *Cas-L* genomic region that contains exon 2 encoding the N-terminal SH3 domain in the Cas-L protein was replaced with EGFP and a neomycin resistance cassette by homologous recombination in ES cells. EGFP was introduced into the exon to generate a fusion protein (Fig. 1*A*). Correct integration of the targeting vector into the *Cas-L* genomic locus was identified by PCR and Southern blot analysis. Two ES cell lines with successful homologous recombination were used to generate chimeric mice and mutant mouse lines were established through germ-line transmission. The mutant loci were confirmed by Southern blot analysis of DNA isolated from the tale (Fig. 1*B*). Western blot analysis of cell lysates from the thymus showed a loss of Cas-L protein in mutant mice, although the possibility remains that truncated Cas-L proteins lacking the exon 2-dependent sequence were not detected (Fig. 1*C*). *Cas-L* mutant (*Cas-L*$^{-/-}$) mice were born with the expected Mendelian frequency and were apparently indistinguishable from wild-type littermates.

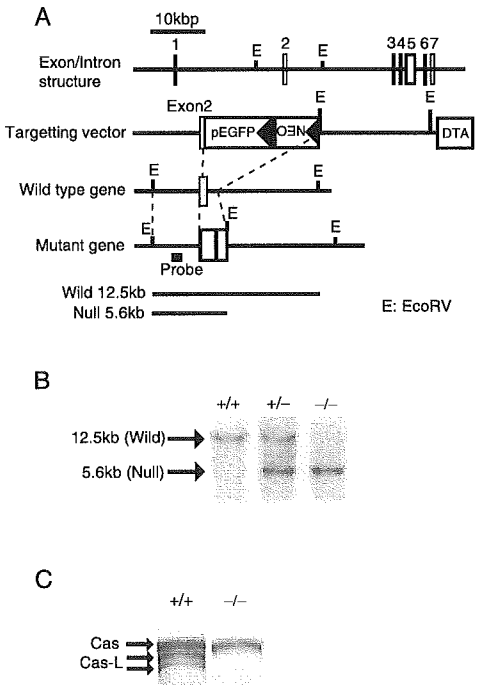

FIGURE 1. Generation of *Cas-L* mutant mice. *A*, Gene-targeting strategy. The exon coding the SH3 domain of *Cas-L* was replaced by EGFP and the neomycin resistance gene (Neo). The length of each diagnostic fragment and the probe position for Southern blotting are indicated. Restriction enzyme *Eco*RV was used for diagnosis. *B*, Southern blot analysis. Genomic DNA from the tails of wild-type (+/+), heterozygous (+/−), and homozygous (−/−) mice were digested with *Eco*RV. Hybridizations were performed with the probe shown in *A*. *C*, Western blot analysis. Proteins from thymi of wild-type and *Cas-L*$^{-/-}$ mice were examined by Western blot analysis using human enhancer of filamentation 1 mAb. The most slowly migrating band indicates Cas protein, whereas two faster migrating bands represent Cas-L proteins.

Reduced lymphocytes in peripheral lymphoid organs from Cas-L$^{-/-}$ *mice*

Because Cas-L is preferentially expressed in lymphocytes (2), we first examined peripheral lymphocyte populations in *Cas-L*$^{-/-}$ mice. *Cas-L*$^{-/-}$ mice had normal numbers of peripheral blood cells, which showed no morphological abnormality (Fig. 2*A*). No obvious alteration in the B or T cell populations was observed. Subsequent analyses of splenocytes showed a significant reduction of the total lymphocyte number, to ~50% of that in wild-type mice (Fig. 2*B*). Both B cell and T cell numbers in the spleen were significantly diminished in the absence of Cas-L. The ratio of T cells to B cells in the spleen was increased, which showed that B cells were more affected than T cells (data not shown). The populations of T and B cells in the lymph nodes were also investigated. The total number of lymphocytes and the numbers of T and B cells in *Cas-L*$^{-/-}$ were significantly reduced compared with those in wild-type mice (Fig. 2*C*). T cell subsets in the peripheral blood and secondary lymphoid tissues were assessed by measuring the cell surface expression of CD4 and CD8. The results showed a normal ratio of CD4 to CD8 in the mutant mice (data not shown). To examine whether these reductions result from abnormal hemopoiesis in the bone marrow, we analyzed the total cell number and

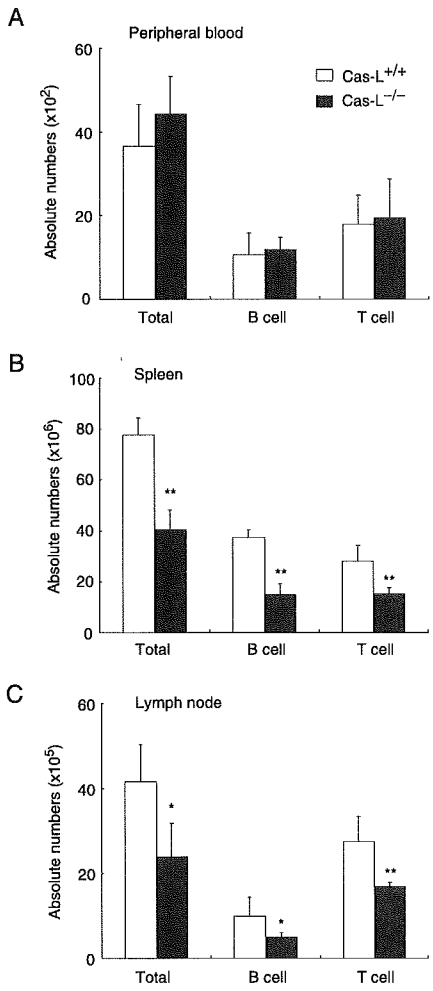

FIGURE 2. Peripheral lymphocyte population in Cas-L-deficient mice. Cells from peripheral blood (*A*), spleen (*B*), and lymph nodes (*C*) were collected from 8- to 10-wk-old mice and counted. B and T cell subsets were stained for CD19 and TCR-β, respectively, and analyzed by FACS. Data are mean ± SD from the experiments using seven mice. *, $p < 0.05$ and **, $p < 0.01$ analyzed with Student's t test.

B cell population in the bone marrow based on the criteria of Hardy et al. (35). The findings revealed no difference in the number of B cell subsets, suggesting that early B cell development was intact in the mutant mice (Table I). As for the thymus, no abnormality was detected in CD4 or CD8 single positive cell populations (data not shown). Taken together, these results indicate that Cas-L affects normal homeostasis in peripheral lymphoid compartments.

MZB cell defect in Cas-L-deficient mice

Because initial analyses showed a striking reduction in the number of B cells in the spleen of *Cas-L*$^{-/-}$ mice, late B cell development in the spleen was investigated. We examined the cell surface expression of CD21 and CD23 to discriminate among newly formed B cells (B220^{+}CD21^{low}CD23^{low}), FOB cells (B220^{+}CD21^{int} CD23^{high}), and MZB cells (B220^{+}CD21^{high}CD23^{low}). *Cas-L*$^{-/-}$ mice showed a marked decrease in the MZB cell population and a complementary increase in the percentage of FOB cells (Fig. 3*A*). The absolute numbers of both MZB cells and FOB cells were decreased (Table I). We next analyzed the splenic B cell compartment in *Cas-L*$^{-/-}$ mice by measuring other B cell markers, including IgM and IgD. The B220^{+}IgM^{high}IgD^{low} population, which includes MZB cells (21), was also reduced in *Cas-L*$^{-/-}$ mice compared with wild-type mice (Fig. 3*B*, Fraction III type cells, and Table I). To confirm the defect of MZB cells in *Cas-L*$^{-/-}$ mice, the expression of CD1d, which is a distinctive marker of MZB cells (36), was analyzed in B220^{+}IgM^{high}IgD^{low} cells. Decreased CD1d^{high} cell population was found in *Cas-L*$^{-/-}$ mice compared with wild-type mice (Fig. 3*C*). Consistent with the results from flow cytometric analyses, histological examination of the spleen showed that the IgM^{high}IgD^{low} MZB cell number was reduced in the absence of Cas-L (Fig. 3*D*).

MZ is composed of several kinds of cells in addition to MZB cells such as stromal cells and macrophages. The MZB cell defect could result from either cell autonomous impairment or an incomplete microenvironment that supports B cell differentiation. To determine which possibility is more likely in *Cas-L*$^{-/-}$ mice, we examined the reconstitution of MZB cells after reciprocal cell transfer between wild-type mice and *Cas-L*$^{-/-}$ mice. The transfer of Cas-L-deficient bone marrow into sublethally irradiated congenic wild-type hosts did not result in the reconstitution of MZB cells (Fig. 4, *middle panel*). In contrast, the transfer of bone marrow cells from wild-type mice into sublethally irradiated *Cas-L*$^{-/-}$ recipients resulted in the generation of normal MZB cell population (Fig. 4, *right panel*). Thus, these results demonstrated that Cas-L is integral for the maintenance of MZB cells and that the defect of MZB cells in these mice is intrinsic to *Cas-L*$^{-/-}$ B cells.

BCR-mediated signaling and immune responses in the absence of Cas-L

Among a number of reports that analyzed the mechanism of the MZB cell deficit, some reports have indicated that the absence of MZB cells arises from enhanced BCR signaling (21, 23). Cas-L is also suggested to be involved in BCR-mediated signal transduction (17). Therefore the defect of MZB cells in *Cas-L*$^{-/-}$ mice might result from aberrant BCR signaling. To test this issue, Ca^{2+} mobilization assays were performed. The results showed that the extent of Ca^{2+} flux in *Cas-L*$^{-/-}$ B cells was slightly decreased compared with that in wild-type B cells (Fig. 5*A*). We next investigated the mitogenic responses of *Cas-L*$^{-/-}$ splenic B cells. The proliferations of *Cas-L*$^{-/-}$ B cells in response to graded concentrations of anti-IgM were comparable to those of the control cells (Fig. 5*B*). Moreover, no significant differences were observed in the proliferation resulting from the combination of anti-IgM, anti-CD40, or IL-4 (Fig. 5*C*).

In addition, we analyzed the involvement of Cas-L in the humoral immune response. The measurements of Ig isotype levels in the serum from nonimmunized *Cas-L*$^{-/-}$ mice showed a decrease in IgG2a compared with the serum from wild-type mice (Fig. 5*D*). Subsequently, we immunized mice against TNP-conjugated KLH, which is a T cell-dependent Ag. The concentrations of TNP-specific Abs in *Cas-L*$^{-/-}$ mice revealed a normal response to the T cell-dependent Ag (Fig. 5*E*). Because MZB cells are indicated to be involved in the T cell-independent Ab response against phosphorylcholine (37), we next examined the levels of anti-phosphorylcholine Abs after immunization with *S. pneumoniae* strain R36A. The slightly reduced level of phosphorylcholine-specific IgM was detected in *Cas-L*$^{-/-}$ mice (Fig. 5*F*), which is compatible with the decreased number of MZB cell, although other Ig isotype levels in *Cas-L*$^{-/-}$ mice were comparable to those in wild-type mice (data not shown). Taking these findings together, the defect of MZB cells in *Cas-L*$^{-/-}$ mice is unlikely to be caused mainly by enhanced BCR signaling.

Table I. *B cell populations in Cas-L-deficient mice*[a]

Tissue	Cell Type	Cas-L$^{+/+}$	Cas-L$^{-/-}$
Spleen	Total B cells	37.4 ± 3.0 (×10^{6}/ml)	15.0 ± 4.1** (×10^{6}/ml)
	NFB cells	3.0 ± 0.8	1.2 ± 0.5**
	FOB cells	25.6 ± 7.5	11.9 ± 4.9*
	MZB cells	1.63 ± 0.2	0.2 ± 0.05**
	Fraction I	14.1 ± 4.5	6.3 ± 1.9**
	Fraction II	7.1 ± 1.8	3.6 ± 1.6**
	Fraction III	6.8 ± 1.7	2.1 ± 0.9**
Bone marrow	Total B cells	22.3 ± 6.2 (×10^{5}/ml)	25.1 ± 8.2 (×10^{5}/ml)
	Fraction A–C	2.6 ± 0.7	3.5 ± 1.0
	Fraction D	9.1 ± 3.7	9.7 ± 4.1
	Fraction E	3.2 ± 1.6	2.7 ± 1.2
	Fraction F	3.5 ± 1.8	4.5 ± 2.1
Lymph nodes	Total B cells	9.9 ± 4.5 (×10^{5}/ml)	5.0 ± 1.1* (×10^{5}/ml)
Peripheral blood	Total B cells	10.5 ± 5.4 (×10^{2}/ml)	11.8 ± 2.9 (×10^{2}/ml)

[a] Cells from the spleen, bone marrow, lymph nodes, and peripheral blood were stained with appropriate B cell markers, and each cell population was analyzed by FACS. FOB, NFB, and MZB represent follicular B, newly formed B, and marginal zone B cells, respectively. Fraction I, II, and III were defined by IgM^{low}IgD^{high}, IgM^{high}IgD^{high}, and IgM^{high}IgD^{low}, respectively. Fractions A–D were determined using the criteria of Hardy. Data are mean ± SD derived from seven mice except for the subset analysis for the spleen, where data are derived from six mice. *, $p < 0.05$ and **, $p < 0.01$ by Student's *t* test.

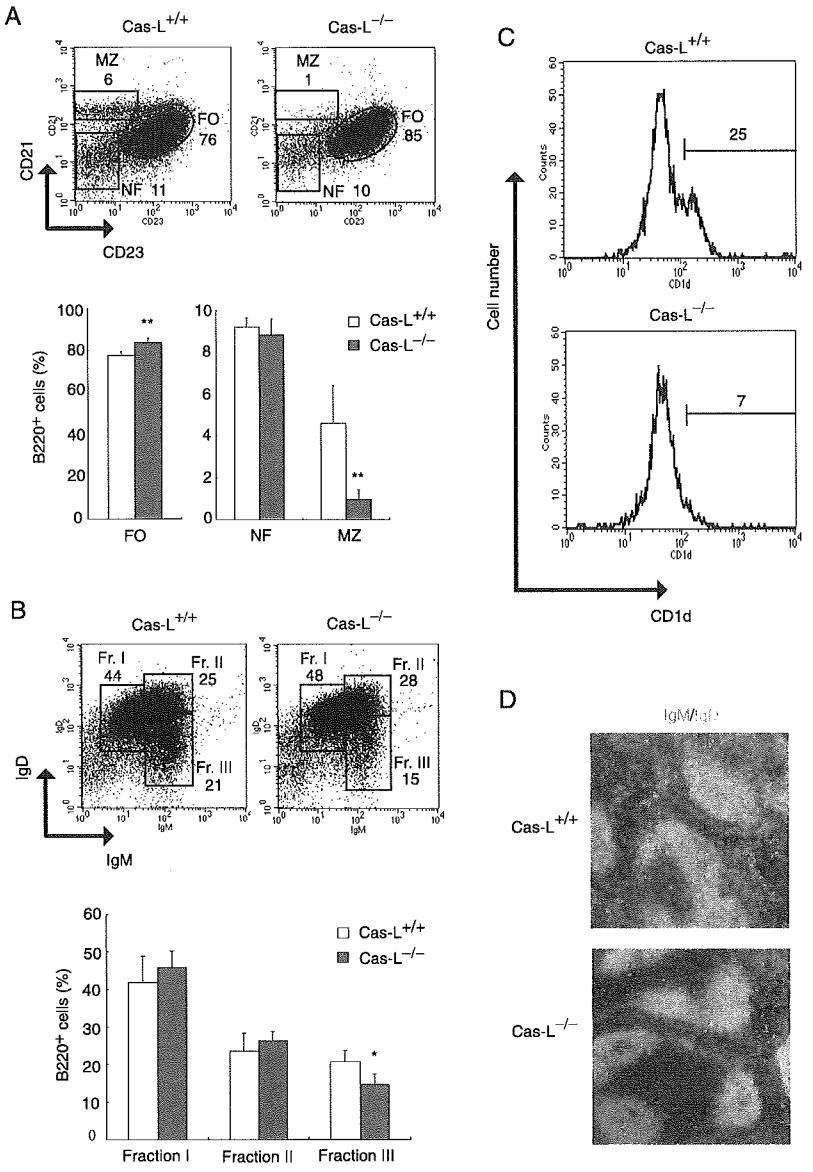

FIGURE 3. MZB cell deficit in the absence of Cas-L. *A* and *B*, FACS analysis of B cell population in spleen. Splenocytes from 8- to 10-wk-old wild-type and *Cas-L*$^{-/-}$ mice were stained for B220, CD21, and CD23 (*A*) and for B220, IgM, and IgD (*B*). The numbers indicate the percentage of each subset in B220^{+} cells. Each subset was also presented by a histogram. MZB (MZ), FOB (FB), and newly formed (NF) B cells are shown. Fraction I, II, and III were defined by IgM^{low}IgD^{high}, IgM^{high}IgD^{high}, and IgM^{high}IgD^{low}, respectively. Data are mean ± SD from three independent experiments using two mice in each case. *, $p < 0.05$ and **, $p < 0.01$, by Student's *t* test. *C*, The reduced number of CD1d^{high} cells in *Cas-L*$^{-/-}$ mice. Splenocytes were also stained for CD1d to confirm the reduction of MZB cells. Values denote the percentages of CD1d^{high} cells among IgM^{high}IgD^{low} B cells. *D*, Immunofluorescent histochemistry of MZB cells. Nonimmunized splenic cryosections were stained with FITC anti-IgD and Alexa Fluor 594 anti-IgM.

Aberrant migration and adhesion in Cas-L-deficient FOB cells

Previous reports had also indicated that the loss of MZB cells can result from altered lymphocyte motility, which presumably causes mal-localization (25–27). Because in vitro assays had shown that Cas-L was involved in cell movement, the loss of MZB cells in *Cas-L*$^{-/-}$ mice might be relevant to the impairment of cell migration. To address this possibility, chemotaxis assays were performed using splenocytes derived from wild-type and *Cas-L*$^{-/-}$ mice. To preclude the effect of the decrease of MZB cells in *Cas-L*$^{-/-}$ mice, we analyzed FOB cells, which account for 80% of splenic B cells and include MZB cell precursors. We examined their migration in response to CXCL12 and CXCL13, which induce a strong chemotactic reaction in peripheral B cells (29, 38). The results showed that the chemotaxis of *Cas-L*$^{-/-}$ FOB cells was decreased in a dose-dependent fashion (Fig. 6, *A* and *B*).

Considering lymphocyte localization, integrins are indispensable molecules and Cas-L plays a crucial role in the integrin-mediated pathway. Among the integrin ligands, VCAM-1 and ICAM-1 are essential for the retention of MZB cells (39). Therefore we investigated the response of *Cas-L*$^{-/-}$ FOB cells to VCAM-1 and ICAM-1 using adhesion assays. As shown in Fig. 6, *C* and *D*, FOB cells from *Cas-L*$^{-/-}$ mice showed attenuated responses to both VCAM-1 and ICAM-1 compared with those from wild-type mice.

We then performed flow cytometric analyses to evaluate the expression level of the relevant receptor for each ligand. Measurements of surface chemokine receptors (CXCR4 and CXCR5, receptors of CXCL12 and CXCL13, respectively) and integrin receptors (integrin α_4 and β_1, subunits of the receptor for VCAM-1, and α_L and β_2, subunits of the receptor for ICAM-1) on splenic B cells or FOB cells from wild-type mice and *Cas-L*$^{-/-}$ mice showed no significant difference in their expression levels (data not shown). Taken together, *Cas-L*$^{-/-}$ FOB cells show perturbed migration and adhesion, which may be associated with the defect of MZB cells.

Cas-L affects lymphocyte trafficking in secondary lymphoid organs

In *Cas-L*$^{-/-}$ mice, another significant finding is the reduced number of lymphocytes in peripheral lymphoid organs. Our findings that migration and adhesion of splenic B cells were impaired in *Cas-L*$^{-/-}$ mice suggest that the aberrant lymphocyte movement may be responsible for this reduction. Previous studies indicated that chemokines (CXCL12, CXCL13, and CCL19/CCL21) and the

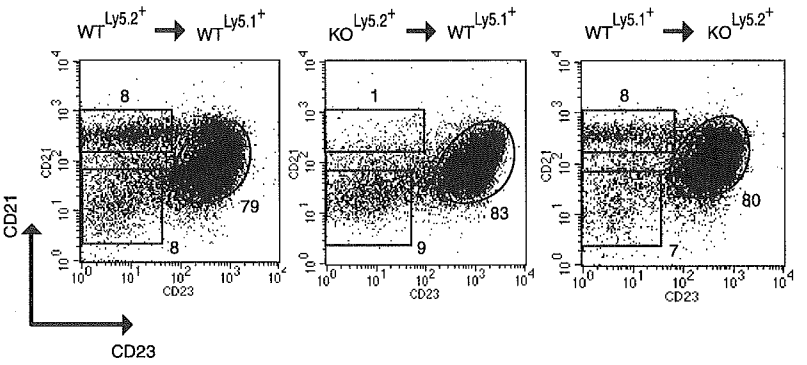

FIGURE 4. MZB cell deficit in *Cas-L*$^{-/-}$ mice is lymphocyte autonomous. Bone marrow cells from wild-type (WT Ly5.2$^+$) or *Cas-L*$^{-/-}$ 10-wk-old mice (KO Ly5.2$^+$) were transferred into lethally irradiated congenic wild-type mice (Ly5.1$^+$) (*left* and *middle panels*). Bone marrow cells from congenic wild-type mice (Ly5.1$^+$) were reciprocally injected into *Cas-L*$^{-/-}$ mice (*right panel*). Twelve weeks later, splenocytes of donor origin were stained for Ly5.1 (or Ly5.2), B220, CD21, and CD23 and analyzed by FACS. Numbers indicate the percentage of gated cells for Ly5.2$^+$ and B220$^+$ cells (*left* and *middle panels*) or for Ly5.1$^+$ and B220$^+$ cells (*right panel*). Data are representatives of three independent experiments using at least two mice in each experiment.

integrin family (VLA-4 and LFA-1, receptors of VCAM-1 and ICAM-1, respectively) have pivotal roles in lymphocyte trafficking in spleen and lymph nodes (30–34). Therefore we first examined chemotaxis and adhesiveness of splenic T cells to determine whether T cells from *Cas-L*$^{-/-}$ mice also show the same inadequate migration and adhesion as *Cas-L*$^{-/-}$ B cells. As shown in Fig. 7, *A* and *B*, the chemotaxis of *Cas-L*$^{-/-}$ T cells to CXCL12 and CCL21, both of which are known to be important chemokines for peripheral T cells (40, 41), was significantly attenuated. The adhesion assay revealed impaired adhesiveness to both VCAM-1

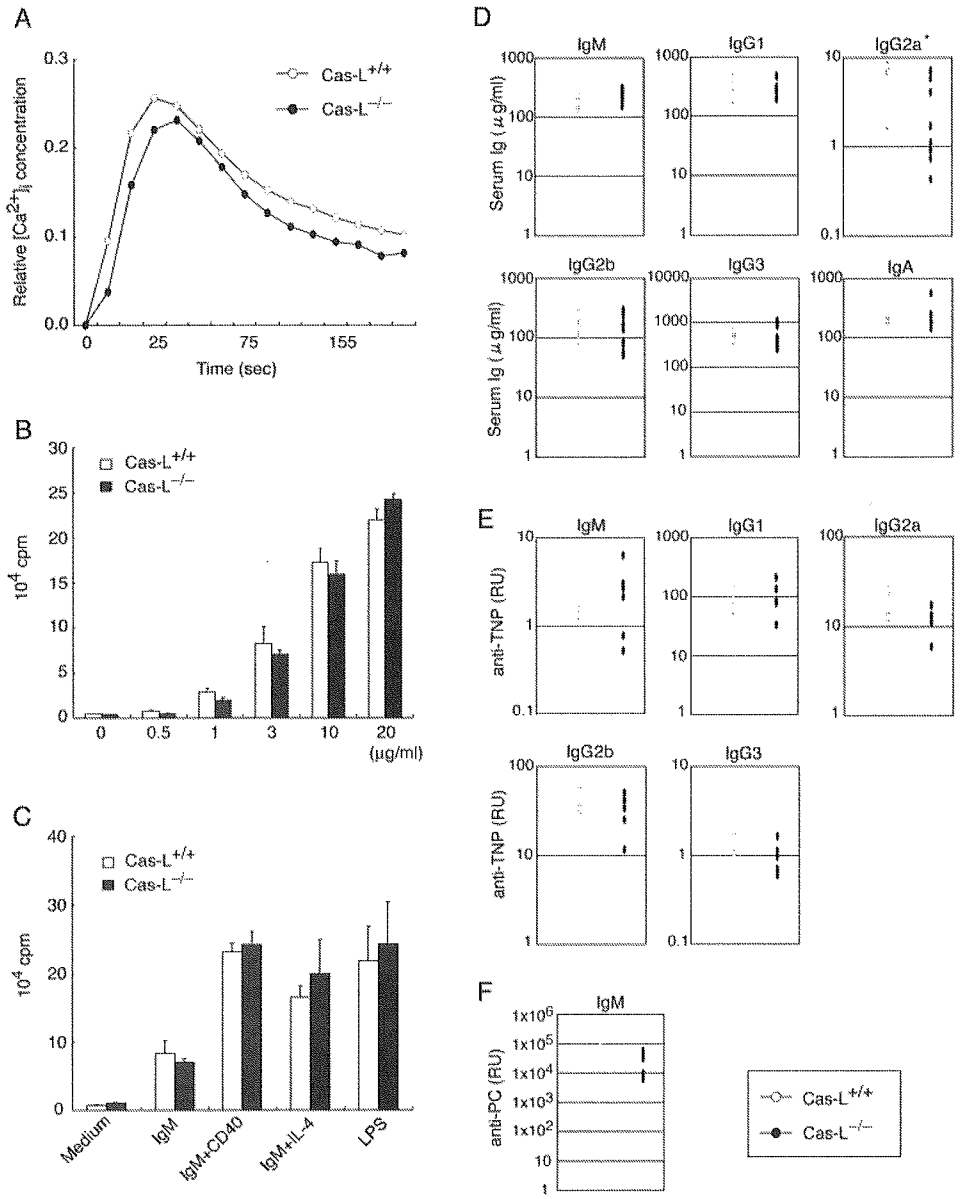

FIGURE 5. Immune responses in Cas-L-deficient mice. *A*, BCR-mediated signaling in the absence of Cas-L. Wild-type and *Cas-L*$^{-/-}$ B cells were loaded with Indo-1. The panel shows the changes of intracellular calcium concentration ($[Ca^{2+}]_i$) in B220-gated cells after stimulation with anti-IgM F(ab′)$_2$ (10 μg/ml). Data are expressed as the ratio to the beginning concentration level. A representative of at least three independent experiments is shown. *B* and *C*, BCR- and LPS-mediated proliferation of splenic B cells. Proliferation of wild-type or *Cas-L*$^{-/-}$ B cells was examined by measuring [^{3}H]thymidine incorporation after stimulation with the indicated doses of anti-IgM F(ab′)$_2$ (*B*). The assay was also performed with the combination of anti-IgM F(ab′)$_2$ (3 μg/ml), anti-CD40 (5 μg/ml), mouse IL-4 (10 ng/ml), and LPS (20 μg/ml). The panel is representative of at least three independent experiments. *D*, Serum Ig concentrations in nonimmunized mice. Serum Ig levels in 8- to 9-wk-old wild-type and *Cas-L*$^{-/-}$ mice were measured by ELISA. Each point represents the value obtained from one mouse. *, $p < 0.05$ in Mann-Whitney *U* test. *E*, Humoral responses to T cell-dependent (TD) Ag. Seven- to 8-wk-old mice were immunized with TNP-KLH. Secondary immunization was given at day 21. TNP-specific Abs were measured in serum collected at day 28 after the initial immunization. *F*, Immune response against phosphorylcholine (PC). Ten- to 12-wk-old mice were immunized with *S. pneumoniae* strain R36A. Serum titers of anti-phosphorylcholine-specific IgM were analyzed 7 days after immunization. Data in *E* and *F* were derived from six mice per genotype. *, $p < 0.05$ by Mann-Whitney *U* test.

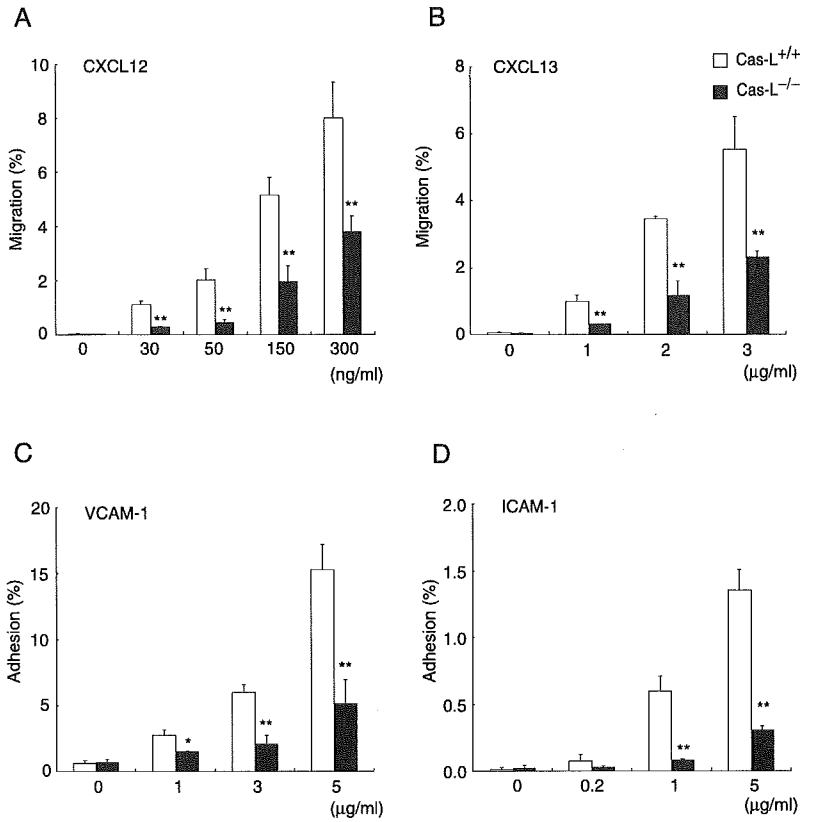

FIGURE 6. Altered B cell movement in Cas-L-deficient mice. *A* and *B*, Migration of *Cas-L*$^{-/-}$ FOB cells. Splenocytes from 8- to 10-wk-old wild-type and *Cas-L*$^{-/-}$ mice stained with CD21, CD23, and B220 were compared in a Transwell chemotaxis assay with the indicated concentrations of CXCL12 (*A*) or CXCL13 (*B*). Cell types were counted before and after migration by FACS. Results are indicated as percentages of migrated FOB cells (B220^{+}CD21^{int}CD23^{high}) for the input FOB cells. *, $p < 0.05$ by Student's *t* test. *C* and *D*, The adhesion ability in *Cas-L*$^{-/-}$ FOB cells. Splenocytes were stained for CD21, CD23, and B220. After incubation with different titers of VCAM-1 (*C*) or ICAM-1 (*D*), FOB cells among adherent cells were counted by FACS. Data shown are the ratio of adherent FOB cells to input FOB cells. Values are mean ± SD from three per group, and data are representative of at least three experiments. *, $p < 0.05$ by Student's *t* test.

and ICAM-1 in *Cas-L*$^{-/-}$ T cells compared with control cells (Fig. 7, *C* and *D*).

Given the impaired migration and adhesion of *Cas-L*$^{-/-}$ B and T cells, we performed trafficking assays in vivo to determine whether lymphocytes in *Cas-L*$^{-/-}$ mice might show altered cell movement in spleen and lymph nodes. Splenocytes isolated from wild-type and *Cas-L*$^{-/-}$ mice (Ly5.2^{+}), which were labeled with BCECF only for *Cas-L*$^{-/-}$ cells, were mixed equally and injected

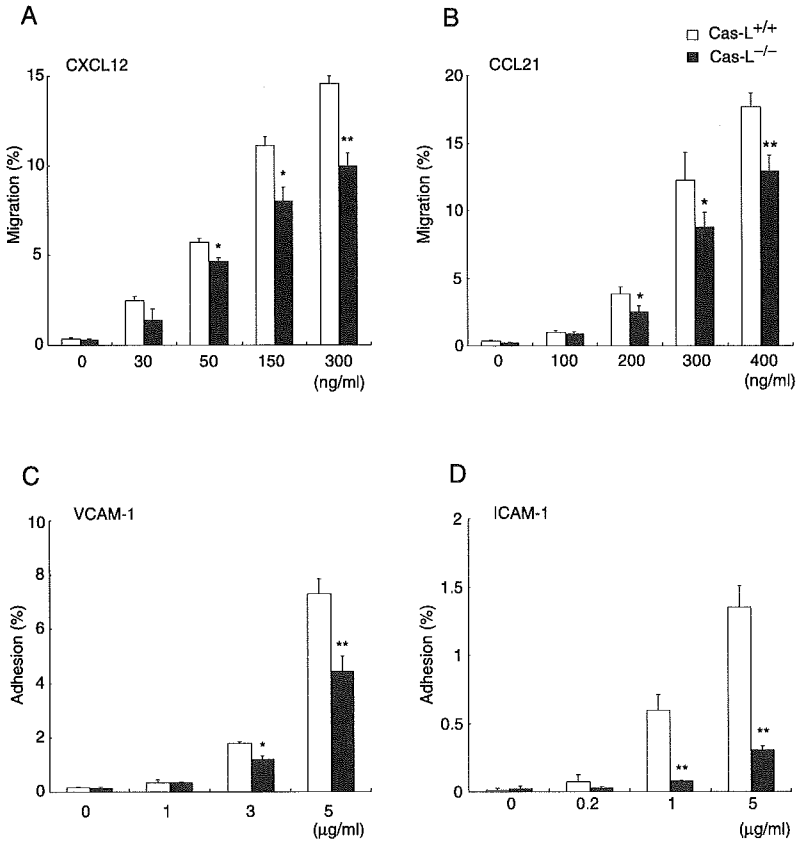

FIGURE 7. Aberrant T cell migration and adhesion in Cas-L-deficient mice. *A* and *B*, Migration of *Cas-L*$^{-/-}$ T cells. Splenocytes from wild-type and *Cas-L*$^{-/-}$ mice stained for Thy1.2 and B220 were compared in a transwell chemotaxis assay with the indicated concentrations of CXCL12 (*A*) or CCL21 (*B*). Data are presented as the ratio of migrated T cells to input T cells. *, $p < 0.05$ by Student's *t* test. *C* and *D*, The adhesion ability in *Cas-L*$^{-/-}$ T cells. Splenocytes were stained for Thy 1.2 and B220. After incubation with VCAM-1 (*C*) or ICAM-1 (*D*), the number of T cells included in the adherent cells was counted by FACS. Data show the ratio of adherent T cells to input T cells. Values are mean ± SD from three per group, and data are representative of at least three experiments. *, $p < 0.05$ by Student's *t* test.

into congenic wild-type mice (Ly5.1$^+$). Forty-eight hours after injection, splenocytes were harvested and host cells were separated from donor cells using Ly5.1. *Cas-L*$^{-/-}$ cells were discriminated from wild-type cells by the marker BCECF (Fig. 8*A*). Peripheral lymph nodes and peripheral blood were also analyzed in the same way. The number of homing *Cas-L*$^{-/-}$ cells showed a modest but significant decrease in both the spleen and lymph nodes (Fig. 8, *A* and *B*). In contrast, the ratios of total lymphocytes and B cells in peripheral blood derived from *Cas-L*$^{-/-}$ mice were elevated, although the change in the T cell ratio was not statistically significant (Fig. 8*C*). Thus, these results suggest the possibility that the reduction in the number of lymphocytes in spleen and lymph nodes of *Cas-L*$^{-/-}$ mice is due to altered lymphocyte trafficking.

Discussion

Cas-L-deficient mice have defective MZB cells, although other subsets of splenic B cells show an almost normal pattern. On the basis of previous reports, we addressed two possible reasons for this defect: distorted localization of MZB cells and impairment of MZB cell differentiation.

The first hypothesis is suggested by data indicating alteration of the migratory ability in gene-targeted mice lacking Pyk-2 or DOCK2 (25, 27). These proteins function as important mediators of G protein-coupled chemokine receptor signal transduction. A previous study showed that pertussis toxin, a Gαi inhibitor, causes the disappearance of MZB cells, suggesting that aberrant chemokine receptor signaling could give rise to defective MZB cells (27). In Cas-L-deficient mice, a decreased chemotactic response is also detected, although no obvious correlation between Cas-L and chemokine receptors has yet been reported. Taken together with our demonstration that Cas-L regulates not only integrin-mediated but also chemokine-mediated cell motility, Cas-L could have a function in the signal pathway from G protein-coupled chemokine receptor.

Gene-disrupted mice lacking DOCK2, a key molecule of chemokine-mediated Rac activation, showed complete loss of chemotactic responses, which would result in the defect of MZB cells. In Cas-L-deficient mice, however, the response to chemokines is reduced to ~50% of that seen in wild-type mice. Therefore, it would appear that abnormal chemotaxis is not enough to explain the marked reduction of MZB cells in *Cas-L*$^{-/-}$ mice. Although previous studies have stressed altered chemotactic activity to explain the absence of MZB cells, cell lodgment to the lymphoid-specific region is controlled not only by migration but also by adhesion. Significant in this regard is our observation that *Cas-L*$^{-/-}$ B cells have the impaired ability to adhere to VCAM-1 and ICAM-1, both of which are known to be indispensable molecules for the adhesion of MZB cells. In the current study, we first demonstrated that the

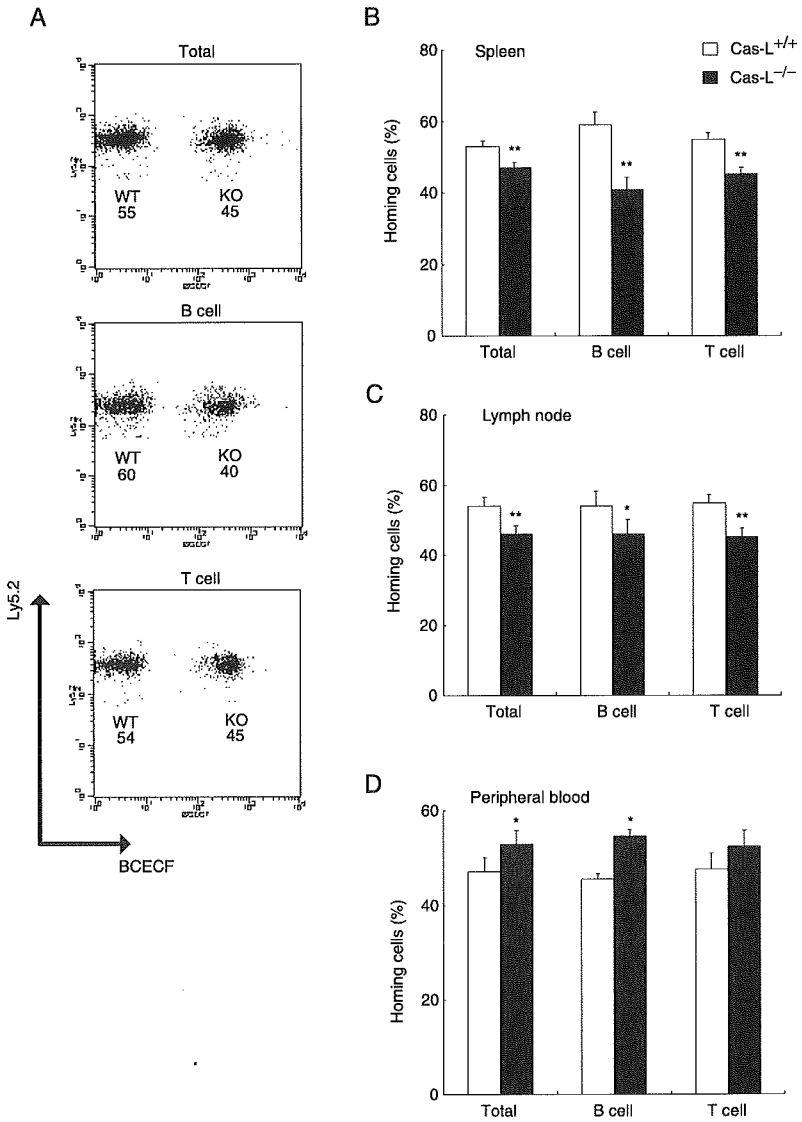

FIGURE 8. Aberrant lymphocyte trafficking in *Cas-L*$^{-/-}$ mice. BCECF-labeled splenocytes from *Cas-L*$^{-/-}$ mice (KO) were mixed with unlabeled splenocytes from wild-type (WT) mice. Both cells (Ly5.2$^+$) were injected into congenic recipient mice (Ly5.1$^+$). Forty-eight hours later, spleens, lymph nodes, and peripheral blood were harvested. Ly5.2$^+$ cells in the spleen were selected and the ratio of *Cas-L*$^{-/-}$ cells (BCECF$^+$ cells) and wild-type cells (BCECF$^-$ cells) detected in the transferred cells were presented (*A*). Data are mean ± SD from three independent experiments using two mice in each case (*B*). The assays were also performed for lymph nodes (*C*) and peripheral blood (*D*). *, $p < 0.05$ and **, $p < 0.01$ by Student's *t* test.

defect of MZB cells may result from abnormalities in both migration and adhesion. These findings are also consistent with the previous reports that Cas-L functions in the pathway mediated by β_1 integrin, a receptor subset for VCAM-1. In contrast, no previous studies have clarified a correlation between Cas-L and LFA-1, which was suggested by our observation that Cas-L is required for the signaling from LFA-1.

Although our findings suggest that Cas-L is indispensable for lymphocyte localization in MZB, they do not preclude the possibility that MZB cell development is perturbed in *Cas-L*$^{-/-}$ mice. Previous studies have indicated the involvement of signaling from BCR and Notch2 in MZB cell differentiation, both of which are membrane-bound receptors distinctly expressed on B cells. The former leads to a hypothesis that enhanced BCR signaling causes loss of MZB cells, although this remains disputable (42, 43). In this regard, Cas-L is suggested to commit to BCR signaling through association with Lyn, which negatively regulates BCR signaling by mediating inhibitory signals from CD22 and FcγRIIb (44, 45). Interestingly, previous studies reported that the absence of Lyn or CD22 resulted in loss of MZB cells with hypersensitive BCR signaling (23, 46). From these findings, we expected *Cas-L*$^{-/-}$ B cells to show enhanced BCR signal intensity. Our data, however, showed no evidence of BCR signal enhancement. Recent studies have suggested that the Notch2 signal pathway plays a pivotal role in determining MZB cell differentiation fate (22, 24). We analyzed the expression level of Notch2 in FOB cells from *Cas-L*$^{-/-}$ mice using real-time PCR, and found that it showed no obvious difference from that in wild-type B cells (data not shown). Taken as a whole, there is so far no available evidence to suggest aberrant MZB cell differentiation in *Cas-L*$^{-/-}$ mice.

Finally, another important finding in *Cas-L*$^{-/-}$ mice was the contraction of peripheral lymphoid organs. The results of our trafficking assay suggested that this contraction would have resulted from aberrant lymphocyte movement. We also examined other possibilities to explain contraction of secondary lymphoid organs: maturation arrest, insufficient proliferation, and altered cell turnover. With regard to the first possibility, flow cytometric analyses of bone marrow and thymus showed no significant abnormalities in B or T cell development that could account for this reduction (Table I and data not shown). Second, the lymphocyte proliferation assay upon BCR and LPS stimulation revealed no obvious difference between wild-type and *Cas-L*$^{-/-}$ mice (Fig. 5, *B* and *C*). Therefore the scenario of insufficient propagation of lymphocytes is unlikely. To test the third possibility, altered cell turnover, we performed an in vivo BrdU labeling assay (data not shown). The frequencies of BrdU-labeled cells in *Cas-L*$^{-/-}$ mice remained comparable to those in wild-type mice. Furthermore, no remarkable augmentation of apoptotic cells in the Cas-L-deficient spleen was detected in histological evaluation with TUNEL staining or flow cytometric analyses using annexin V assay (data not shown). Taking these findings together, it might be difficult to attribute the decreased number of peripheral lymphocytes to altered cell turnover. Therefore it would appear that lymphocyte reduction in secondary lymphoid organs is mainly due to altered lymphocyte trafficking. Because reduction of cell population is most striking in MZB cells of the spleen, we also analyzed a BCR-mediated response or cell turnover in the MZB cells. Although *Cas-L*$^{-/-}$ MZB cells showed slightly reduced Ca^{2+} flux in the Ca^{2+} mobilization assays or decreased apoptotic cells in the annexin V assay, no significant differences were obtained (data not shown). However, because the number of MZB cells in *Cas-L*$^{-/-}$ mice is very small, a subtle alteration, if any, might not have been detectable.

In summary, using gene-targeted mice, we have demonstrated that Cas-L is integral for both cell migration and adhesion, a lack of which may contribute to a defect of MZB cells in the spleen and contraction of secondary lymphoid organs.

Acknowledgments

We thank S. Aizawa for TT2 ES cells, H. Ito for *S. pneumoniae* strain R36A, S. Kumar for cDNA of Nedd9, and R. Takizawa and Y. Sato for help with the generation and breeding of *Cas-L*$^{-/-}$ mice.

Disclosures

The authors have no financial conflict of interest.

References

1. Law, S. F., J. Estojak, B. Wang, T. Mysliwiec, G. Kruh, and E. A. Golemis. 1996. Human enhancer of filamentation 1, a novel p130cas-like docking protein, associates with focal adhesion kinase and induces pseudohyphal growth in *Saccharomyces cerevisiae*. *Mol. Cell. Biol.* 16: 3327–3337.
2. Minegishi, M., K. Tachibana, T. Sato, S. Iwata, Y. Nojima, and C. Morimoto. 1996. Structure and function of Cas-L, a 105-kD Crk-associated substrate-related protein that is involved in β1 integrin-mediated signaling in lymphocytes. *J. Exp. Med.* 184: 1365–1375.
3. Sakai, R., A. Iwamatsu, N. Hirano, S. Ogawa, T. Tanaka, H. Mano, Y. Yazaki, and H. Hirai. 1994. A novel signaling molecule, p130, forms stable complexes in vivo with v-Crk and v-Src in a tyrosine phosphorylation-dependent manner. *EMBO J.* 13: 3748–3756.
4. Honda, H., H. Oda, T. Nakamoto, Z. Honda, R. Sakai, T. Suzuki, T. Saito, K. Nakamura, K. Nakao, T. Ishikawa, et al. 1998. Cardiovascular anomaly, impaired actin bundling and resistance to Src-induced transformation in mice lacking p130Cas. *Nat. Genet.* 19: 361–365.
5. Giancotti, F. G., and E. Ruoslahti. 1999. Integrin signaling. *Science* 285: 1028–1032.
6. Hynes, R. O. 1987. Integrins: a family of cell surface receptors. *Cell* 48: 549–554.
7. Ruoslahti, E., and J. C. Reed. 1994. Anchorage dependence, integrins, and apoptosis. *Cell* 77: 477–478.
8. Springer, T. A. 1990. Adhesion receptors of the immune system. *Nature* 346: 425–434.
9. Astier, A., S. N. Manié, H. Avraham, H. Hirai, S. F. Law, Y. Zhang, E. A. Golemis, Y. Fu, B. J. Druker, N. Haghayeghi, et al. 1997. The related adhesion focal tyrosine kinase differentially phosphorylates p130Cas and the Cas-like protein, p105HEF1. *J. Biol. Chem.* 272: 19719–19724.
10. Tachibana, K., T. Urano, H. Fujita, Y. Ohashi, K. Kamiguchi, S. Iwata, H. Hirai, and C. Morimoto. 1997. Tyrosine phosphorylation of Crk-associated substrates by focal adhesion kinase: a putative mechanism for the integrin-mediated tyrosine phosphorylation of Crk-associated substrates. *J. Biol. Chem.* 272: 29083–29090.
11. Miyake-Nishijima, R., S. Iwata, S. Saijo, H. Kobayashi, S. Kobayashi, A. Souta-Kuribara, O. Hosono, H. Kawasaki, H. Tanaka, E. Ikeda, et al. 2003. Role of Crk-associated substrate lymphocyte type in the pathophysiology of rheumatoid arthritis in tax transgenic mice and in humans. *Arthritis Rheum.* 48: 1890–1900.
12. Ohashi, Y., S. Iwata, K. Kamiguchi, and C. Morimoto. 1999. Tyrosine phosphorylation of Crk-associated substrate lymphocyte-type is a critical element in TCR- and β_1 integrin-induced T lymphocyte migration. *J. Immunol.* 163: 3727–3734.
13. van Seventer, G. A., H. J. Salmen, S. F. Law, G. M. O'Neill, M. M. Mullen, A. M. Franz, S. B. Kanner, E. A. Golemis, and J. M. van Seventer. 2001. Focal adhesion kinase regulates β_1 integrin-dependent T cell migration through an HEF1 effector pathway. *Eur. J. Immunol.* 31: 1417–1427.
14. Sakakibara, A., Y. Ohba, K. Kurokawa, M. Matsuda, and S. Hattori. 2002. Novel function of Chat in controlling cell adhesion via Cas-Crk-C3G-pathway-mediated Rap1 activation. *J. Cell Sci.* 115: 4915–4924.
15. Kanda, H., T. Mimura, N. Morino, K. Hamasaki, T. Nakamoto, H. Hirai, C. Morimoto, Y. Yazaki, and Y. Nojima. 1997. Ligation of the T cell antigen receptor induces tyrosine phosphorylation of p105CasL, a member of the p130Cas-related docking protein family, and its subsequent binding to the Src homology 2 domain of c-Crk. *Eur. J. Immunol.* 27: 2113–2117.
16. Kanda, H., T. Mimura, K. Hamasaki, K. Yamamoto, Y. Yazaki, H. Hirai, and Y. Nojima. 1999. Fyn and Lck tyrosine kinases regulate tyrosine phosphorylation of p105CasL, a member of the p130Cas docking protein family, in T-cell receptor-mediated signalling. *Immunology* 97: 56–61.
17. Manié, S. N., A. R. P. Beck, A. Astier, S. F. Law, T. Canty, H. Hirai, B. J. Druker, H. Avraham, N. Haghayeghi, M. Sattler, et al. 1997. Involvement of $p130^{Cas}$ and p105(HEF1), a novel Cas-like docking protein, in a cytoskeleton-dependent signaling pathway initiated by ligation of integrin or antigen receptor on human B cells. *J. Biol. Chem.* 272: 4230–4236.
18. Zhang, Z., L. Hernandez-Lagunas, W. C. Horne, and R. Baron. 1999. Cytoskeleton-dependent tyrosine phosphorylation of the $p130^{Cas}$ family member HEF1 downstream of the G protein-coupled calcitonin receptor.: calcitonin induces the association of HEF1, paxillin, and focal adhesion kinase. *J. Biol. Chem.* 274: 25093–25098.
19. Pillai, S. 1999. The chosen few? Positive selection and the generation of naive B lymphocytes. *Immunity* 10: 493–502.
20. Oliver, A. M., F. Martin, and J. F. Kearney. 1999. $IgM^{high}CD21^{high}$ lymphocytes enriched in the splenic marginal zone generate effector cells more rapidly than the bulk of follicular B cells. *J. Immunol.* 162: 7198–7207.

21. Cariappa, A., M. Tang, C. Parng, E. Nebelitskiy, M. Carroll, K. Georgopoulos, and S. Pillai. 2001. The follicular versus marginal zone B lymphocyte cell fate decision is regulated by Aiolos, Btk, and CD21. *Immunity* 14: 603–615.
22. Saito, T., S. Chiba, M. Ichikawa, A. Kunisato, T. Asai, K. Shimizu, T. Yamaguchi, G. Yamamoto, S. Seo, K. Kumano, et al. 2003. Notch2 is preferentially expressed in mature B cells and indispensable for marginal zone B lineage development. *Immunity* 18: 675–685.
23. Seo, S., J. Buckler, and J. Erikson. 2001. Novel roles for Lyn in B cell migration and lipopolysaccharide responsiveness revealed using anti-double-stranded DNA Ig transgenic mice. *J. Immunol.* 166: 3710–3716.
24. Tanigaki, K., H. Han, N. Yamamoto, K. Tashiro, M. Ikegawa, K. Kuroda, A. Suzuki, T. Nakano, and T. Honjo. 2002. Notch-RBP-J signaling is involved in cell fate determination of marginal zone B cells. *Nat. Immunol.* 3: 443–450.
25. Fukui, Y., O. Hashimoto, T. Sanui, T. Oono, H. Koga, M. Abe, A. Inayoshi, M. Noda, M. Oike, T. Shirai, and T. Sasazuki. 2001. Haematopoietic cell-specific CDM family protein DOCK2 is essential for lymphocyte migration. *Nature* 412: 826–831.
26. Girkontaite, I., K. Missy, V. Sakk, A. Harenberg, K. Tedford, T. Pötzel, K. Pfeffer, and K.-D. Fischer. 2001. Lsc is required for marginal zone B cells, regulation of lymphocyte motility and immune responses. *Nat. Immunol.* 2: 855–862.
27. Guinamard, R., M. Okigaki, J. Schlessinger, and J. V. Ravetch. 2000. Absence of marginal zone B cells in Pyk-2-deficient mice defines their role in the humoral response. *Nat. Immunol.* 1: 31–36.
28. Butcher, E. C., and L. J. Picker. 1996. Lymphocyte homing and homeostasis. *Science* 272: 60–66.
29. Bleul, C. C., R. C. Fuhlbrigge, J. M. Casasnovas, A. Aiuti, and T. A. Springer. 1996. A highly efficacious lymphocyte chemoattractant, stromal cell-derived factor 1 (SDF-1). *J. Exp. Med.* 184: 1101–1109.
30. Hargreaves, D. C., P. L. Hyman, T. T. Lu, V. N. Ngo, A. Bidgol, G. Suzuki, Y. R. Zou, D. R. Littman, and J. G. Cyster. 2001. A coordinated change in chemokine responsiveness guides plasma cell movements. *J. Exp. Med.* 194: 45–56.
31. Ansel, K. M., V. N. Ngo, P. L. Hyman, S. A. Luther, R. Forster, J. D. Sedgwick, J. L. Browning, M. Lipp, and J. G. Cyster. 2000. A chemokine-driven positive feedback loop organizes lymphoid follicles. *Nature* 406: 309–314.
32. Andrew, D. P., J. P. Spellberg, H. Takimoto, R. Schmits, T. W. Mak, and M. M. Zukowski. 1998. Transendothelial migration and trafficking of leukocytes in LFA-1-deficient mice. *Eur. J. Immunol.* 28: 1959–1969.
33. Berlin-Rufenach, C., F. Otto, M. Mathies, J. Westermann, M. J. Owen, A. Hamann, and N. Hogg. 1999. Lymphocyte migration in lymphocyte function-associated antigen (LFA)-1-deficient mice. *J. Exp. Med.* 189: 1467–1478.
34. Lo, C. G., T. T. Lu, and J. G. Cyster. 2003. Integrin-dependence of lymphocyte entry into the splenic white pulp. *J. Exp. Med.* 197: 353–361.
35. Hardy, R. R., C. E. Carmack, S. A. Shinton, J. D. Kemp, and K. Hayakawa. 1991. Resolution and characterization of pro-B and pre-pro-B cell stages in normal mouse bone marrow. *J. Exp. Med.* 173: 1213–1225.
36. Roark, J. H., S. H. Park, J. Jayawardena, U. Kavita, M. Shannon, and A. Bendelac. 1998. CD1.1 expression by mouse antigen-presenting cells and marginal zone B cells. *J. Immunol.* 160: 3121–3127.
37. Martin, F., A. M. Oliver, and J. F. Kearney. 2001. Marginal zone and B1 B cells unite in the early response against T-independent blood-borne particulate antigens. *Immunity* 14: 617–629.
38. Gunn, M. D., V. N. Ngo, K. M. Ansel, E. H. Ekland, J. G. Cyster, and L. T. Williams. 1998. A B-cell-homing chemokine made in lymphoid follicles activates Burkitt's lymphoma receptor-1. *Nature* 391: 799–803.
39. Lu, T. T., and J. G. Cyster. 2002. Integrin-mediated long-term B cell retention in the splenic marginal zone. *Science* 297: 409–412.
40. Nagira, M., T. Imai, K. Hieshima, J. Kusuda, M. Ridanpää, S. Takagi, M. Nishimura, M. Kakizaki, H. Nomiyama, and O. Yoshie. 1997. Molecular cloning of a novel human CC chemokine secondary lymphoid-tissue chemokine that is a potent chemoattractant for lymphocytes and mapped to chromosome 9p13. *J. Biol. Chem.* 272: 19518–19524.
41. Nagira, M., T. Imai, R. Yoshida, S. Takagi, M. Iwasaki, M. Baba, Y. Tabira, J. Akagi, H. Nomiyama, and O. Yoshie. 1998. A lymphocyte-specific CC chemokine, secondary lymphoid tissue chemokine (SLC), is a highly efficient chemoattractant for B cells and activated T cells. *Eur. J. Immunol.* 28: 1516–1523.
42. Clayton, E., G. Bardi, S. E. Bell, D. Chantry, C. P. Downes, A. Gray, L. A. Humphries, D. Rawlings, H. Reynolds, E. Vigorito, and M. Turner. 2002. A crucial role for the p110δ subunit of phosphatidylinositol 3-kinase in B cell development and activation. *J. Exp. Med.* 196: 753–763.
43. Martin, F., and J. F. Kearney. 2000. Positive selection from newly formed to marginal zone B cells depends on the rate of clonal production, CD19, and btk. *Immunity* 12: 39–49.
44. Chan, V. W., C. A. Lowell, and A. L. DeFranco. 1998. Defective negative regulation of antigen receptor signaling in Lyn-deficient B lymphocytes. *Curr. Biol.* 8: 545–553.
45. Smith, K. G., D. M. Tarlinton, G. M. Doody, M. L. Hibbs, and D. T. Fearon. 1998. Inhibition of the B cell by CD22: a requirement for Lyn. *J. Exp. Med.* 187: 807–811.
46. Samardzic, T., D. Marinkovic, C.-P. Danzer, J. Gerlach, L. Nitschke, and T. Wirth. 2002. Reduction of marginal zone B cells in CD22-deficient mice. *Eur. J. Immunol.* 32: 561–567.

The EMBO Journal (2005) 24, 3700–3711 | © 2005 European Molecular Biology Organization | All Rights Reserved 0261-4189/05
www.embojournal.org

THE EMBO JOURNAL

Phosphorylation of ephrin-B1 via the interaction with claudin following cell–cell contact formation

Masamitsu Tanaka, Reiko Kamata and Ryuichi Sakai*

Growth Factor Division, National Cancer Center Research Institute, Tsukiji, Chuo-ku, Tokyo, Japan

The interaction of the Eph family of receptor protein tyrosine kinase and its ligand ephrin family induces bidirectional signaling via the cell–cell contacts. Although most previous studies have focused on the function of Eph–ephrin pathways in the neural system and endothelial cells, this process also occurs in epithelial and cancer cells, of which the biological involvement is poorly understood. We show that ephrin-B1 creates an *in vivo* complex with adjacent claudin1 or claudin4 via the extracellular domains of these proteins. The cytoplasmic domain of ephrin-B1 was phosphorylated on tyrosine residues upon the formation of cell–cell contacts, possibly recognizing an intercellular adhesion of claudins. Phosphorylation of ephrin-B1 induced by claudins was abolished by the treatment with 4-amino-5-(4-chlorophenyl)-7-(t-butyl)pyrazolo[3,4-d]pyrimidine, an inhibitor of the Src family kinases. Moreover, overexpression of ephrin-B1 triggered consequent change in the level of cell–cell adhesion depending on its phosphorylation. These results suggest that ephrin-B1 mediated the cell–cell adhesion of epithelial and cancer cells via a novel Eph receptor-independent mechanism.

The EMBO Journal (2005) **24,** 3700–3711. doi:10.1038/sj.emboj.7600831; Published online 6 October 2005
Subject Categories: signal transduction
Keywords: claudin; Eph; ephrin; tight junction

Introduction

The members of the Eph receptor family can be classified into two groups based on their sequence similarity and preferential binding to a subset of ligands tethered to the cell surface either by a glycosylphosphatidyl inositol anchor (ephrin-A) or a transmembrane domain (ephrin-B). The transmembrane ligand ephrin-B1 has been shown to be phosphorylated on tyrosine residues following contact with the corresponding Eph receptor ectodomain, and to have a receptor-like intrinsic signaling potential leading to transduce reverse signaling (Holland *et al*, 1996; Bruckner *et al*, 1997). At present, two major mechanisms are known to transduce signaling from ephrin-B1 (Kullander and Klein, 2002; Murai and Pasquale, 2003; Poliakov *et al*, 2004). The receptor-induced tyrosine phosphorylation of ephrin-B1 recruits Grb4 SH-adaptor protein. Since Grb4 has three SH3 domains, it could link ephrin-B1 to a vast array of signaling molecules (Cowan and Henkemeyer, 2001). Ephrin-B1 also contains PDZ-binding motif at the carboxyl-terminus, which mediates signals by association with proteins, including some phosphatase and GTPase-activating protein of heterotrimeric G proteins (Torres *et al*, 1998; Lin *et al*, 1999; Lu *et al*, 2001; Palmer *et al*, 2002). Although Eph receptors and ephrins play essential roles for proper axon pathfinding in the nervous system, some members of the Eph receptors and their ligands are expressed in epithelial cells. For example, EphB2, EphB3 and ephrin-B1 are reciprocally expressed along the crypt–villus axis in the small intestine, which controls the cell positioning along the crypt axis (Batlle *et al*, 2002). Moreover, the overexpression of Ephs and ephrins is reported in various tumors of epithelial origin (Brantley-Sieders *et al*, 2004; Surawska *et al*, 2004). However, the biological significance of Eph/ephrin in epithelial cells or carcinomas is still poorly understood.

When ephrin-B1 is overexpressed in the embryos of *Xenopus laevis* at an early developmental stage, the cell–cell adhesion of the blastomeres was significantly reduced, leading to fatal effects for the embryos (Jones *et al*, 1998). However, precise identification of the adhesion molecules involved in this phenomenon is still not clear. In order to examine whether ephrin-B1 mediates cell–cell adhesion in the mammalian epithelial cells as well, we established an MDCK cell line, showing the inducible expression of ephrin-B1 through the addition of doxycycline. The MDCK cells expressing ephrin-B1 at a high level tend to loosen the cell–cell adhesion when the cells are compared without expressing ephrin-B1. These observations led us to focus on assessing whether ephrin-B1 could be a mediator of cell–cell adhesion in epithelial cells. While analyzing the proteins involved in the complex formation with ephrin-B1, we identified claudins, which are the major constituents of the tight junctions of epithelial cells. Tight junctions locate in the most apical parts of the lateral membrane and serve as paracellular barriers to restrict the movement of ions and proteins across cell boundaries. Claudins are tetraspan transmembrane proteins comprising a multi-gene family with more than 20 members, and creating a complex with ZO-1, ZO-2 and ZO-3, which represent plaque structures underlying plasma membranes (Morita *et al*, 1999; Tsukita *et al*, 2001). Moreover, claudins are frequently overexpressed in malignant cells, in which the mature tight-junction strands are not present. However, claudin's functions in such naive-contact carcinoma cells are not clear.

In this study, we describe the physical interaction of ephrin-B1 with claudins. Although ephrin-B1 interacts with claudins on the same cell surface *in cis*, the tyrosine phosphorylation of the cytoplasmic region of ephrin-B1 was found to be markedly enhanced by the cell–cell contact formation in a manner dependent on claudin. The expression of ephrin-B1

*Corresponding author. Growth Factor Division, National Cancer Center Research Institute, 5-1-1 Tsukiji, Chuo-ku, Tokyo 104-0045, Japan.
Tel.: +81 3 3542 2511; Fax: +81 3 3542 8170;
E-mail: rsakai@gan2.res.ncc.go.jp

Received: 26 April 2005; accepted: 9 September 2005; published online: 6 October 2005

 ©2005 European Molecular Biology Organization

stimulates the paracellular permeability in MDCK cells, which depends on the tyrosine phosphorylation of ephrin-B1. This is the first report to show that the extracellular region of ephrin-B1 associates with a protein other than its receptor in the Eph family kinases. These observations provide further evidence for the possibility that ephrin-B1 inhibits the formation of the tight cell–cell adhesion in a wide variety of epithelial and cancer cells regardless of the existence of cognate Eph receptors.

Results

Claudin interacts with the extracellular domain (ECD) of ephrin-B1

In the attempt to identify the proteins associating with ephrin-B1, we initially screened cDNA library constructed from *Xenopus* embryos at an early stage of development by the procedure described in Figure 1A. After several rounds of screening of total 5×10^4 cDNAs, we isolated several independent cDNAs, which encode proteins coimmunoprecipitated with ephrin-B1. Among them, one clone (#12; Figure 1A) was almost identical (97% identical in amino acids) to *Xenopus* claudin4 (CLD4)L1 through the partial DNA sequencing, which is most closely related to CLD4 in mouse and human (Fujita *et al*, 2002). Therefore, we focused our study to examine the interaction of ephrin-B1 with CLD4 and also with claudin1 (CLD1), which is most widely expressed in mammalian tissues among the members of claudin family.

To confirm the physical association between claudins with ephrin-B1, coexpression and immunoprecipitation (IP) analysis was first performed in COS1 cells. It was revealed that ephrin-B1 was co-precipitated with CLD1 by the specific antibody (Figure 1B, lane 1), but not by the normal mouse IgG1 (Figure 1B, lane 2). This result was further confirmed through experiments using the antibodies in reverse order. CLD1 was co-precipitated with ephrin-B1 (Figure 1B, lanes 3 and 4, arrowhead). In addition to CLD1, the stable association of CLD4 with ephrin-B1 was demonstrated using similar experiments (Figure 1B, lanes 5–8). We also examined the association between endogenous claudins and ephrin-B1 using the HT29 colon cancer cell line, where ephrin-B1, CLD1 and CLD4 are highly expressed. CLD1 and CLD4 were co-precipitated with ephrin-B1 from the extract of HT29 cells using the specific antibody, but not by normal goat serum (NGS) (Figure 1C, lanes 1, 2, 5 and 6). Furthermore, ephrin-B1 was co-precipitated with CLD1 or CLD4 using the specific antibodies in HT29 cells, confirming a stable level of interaction among these molecules (Figure 1C, lanes 3, 4, 7, 8). In HT29 cells, claudins and ephrin-B1 were diffusely overlapped in the lateral membrane. On the other hand, in ephrin-B1-expressing MDCK cells, the localization of CLD1 was restricted to the tight junctions where ZO-1 was expressed, while ephrin-B1 showed overlapping, but a wider level of expression along the entire region in the lateral membrane (Figure 1D).

In order to determine the region within CLD1, required for the interaction with ephrin-B1, we generated deletion mutants of CLD1. Difference in the binding affinity of the mutants mainly localized at the cell membrane indicates that the cytoplasmic regions of CLD1 were not involved in the interaction with ephrin-B1 (Figure 2A, #1, 6 and 7). Within mutants localized both in the cytoplasm and cell membrane, the ones possessing the first ECD (ECD1) were tightly bound to ephrin-B1 (Figure 2A, #3 and 8), whereas mutants lacking this domain failed to associate with ephrin-B1 (Figure 2A, #2, 4 and 5), suggesting that ECD1 domain of CLD1 is responsible for binding to ephrin-B1. We also generated the same sets of CLD4 mutants with those of CLD1, and revealed that the same domain of CLD4 was necessary for the association with ephrin-B1 (data not shown). These results were further confirmed by the *in vitro* analysis using GST-tagged CLD1 mutants. The GST-fusion proteins, including each extracellular or cytoplamic domain, were incubated with the lysate of cells expressing ephrin-B1, and the association of the claudin mutant and ephrin-B1 was analyzed. The interaction between ephrin-B1 and CLD1 mutant containing ECD1 (aa 1–103) was confirmed (Figure 2B, GST-ECD1). A similar experiment for GST-tagged ephrin-B1 mutants was also performed. CLD1 interacted with the ECD of ephrin-B1 (ephrin-B1 ECD), but not the transmembrane and cytoplasmic domains (ephrin-B1 cyto) (Figure 2B).

Within the ECD of ephrin-B1, the most amino-terminal region (aa 1–166), ephrin-B1-N was required for the interaction with CLD1, because CLD1 fragment containing ECD1 ($CLD1^{1-103}$, corresponding to #8 in Figure 2A) binds to ephrin-$B1^{\Delta 167-236}$, which lacks a residual region of the ECD of ephrin-B1 (Figure 2C). Moreover, the association of ephrin-$B1^{\Delta 167-236}$ and CLD4 fragment containing ECD1 ($CLD4^{1-103}$) was also observed by similar experiments (data not shown). Therefore, we concluded that ephrin-B1-N did interact with the amino-terminal region of claudins, including the first ECD. As ephrin-B1-N also contains a region essential for interaction with EphB receptors (Himanen *et al*, 2001), we further examined whether EphB2 and claudin competitively bind to ephrin-B1 using EphB2-Fc, which is a fusion protein of the ECD of EphB2 with the Fc region of mouse immunoglobulin. Parent L cells do not express detectable claudins (Furuse *et al*, 1998); therefore, CLD4 was retrovirally transduced in L cells stably expressing ephrin-B1 (L ephrin-B1). When EphB2-Fc was added in the cell culture medium, expression of CLD4 reduced the amount of membrane-bound EphB2-Fc, which was detected by both immunoblotting (IB) analysis and immunostaining (Figure 2D). Moreover, in L cells expressing both ephrin-B1 and CLD1 (L ephrin-B1 CLD1), ephrin-B1, but not CLD1, was pulled by EphB2-Fc, while CLD1 was coimmunoprecipitated with ephrin-B1 from the same cell lysate (data not shown). Therefore, CLD1-bound ephrin-B1 does not seem to associate with EphB2-Fc. These results suggest that EphB2 and claudins may competitively associate with the ECD of ephrin-B1.

Ephrin-B1 is phosphorylated on tyrosine residues in the cytoplasmic domain by the interaction with claudin

When ephrin-B1 is stimulated using EphB2, the cytoplasmic domain of ephrin-B1 is highly phosphorylated on tyrosine residues. As the association of claudin and ephrin-B1 depends on their extracellular regions, we subsequently examined whether the phosphorylation of ephrin-B1 was triggered by the interaction with claudin. The coexpression of ephrin-B1 and CLD1 or CLD4 leads to the tyrosine phosphorylation of ephrin-B1 in COS1 cells (Figure 3A, lanes 2 and 5). However, overexpression of CLD1 mutant, which lacks the binding site with ephrin-B1 (CLD1 ΔECD1, corresponds to #2

©2005 European Molecular Biology Organization

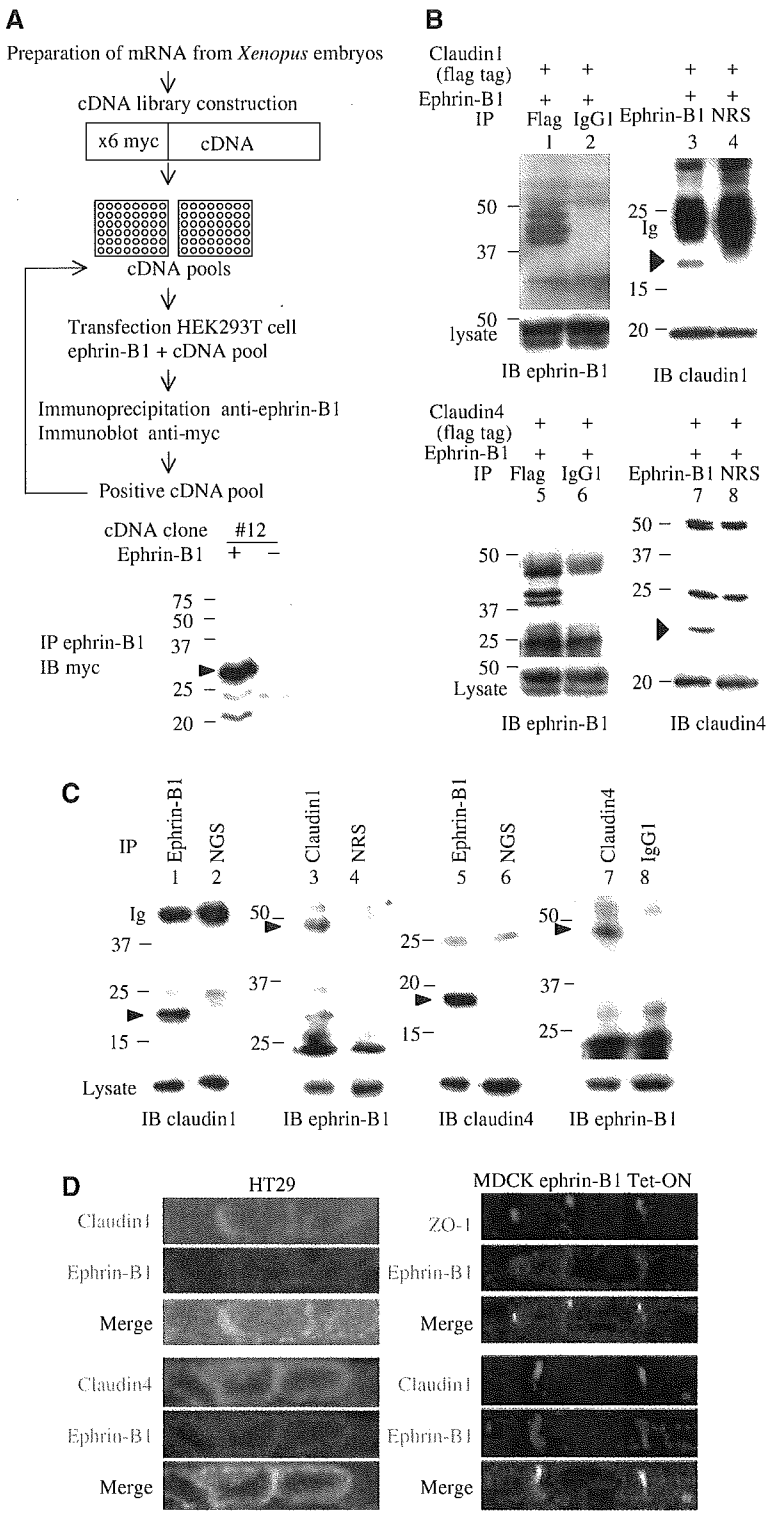

Figure 1 Ephrin-B1 forms a complex with CLD1 and CLD4: (**A**) Schematic outline of cloning procedure for the cDNAs encoding proteins associating with ephrin-B1. A detailed explanation is provided in Materials and methods. (Bottom): A plasmid encoding the cDNA (#12) was transiently transfected into COS1 cells together with or without ephrin-B1. The cell lysates were immunoprecipitated (IP) with an anti-ephrin-B1 antibody, and then subjected to IB with anti-myc antibody. It should be noted that six copies of the myc-epitope tagged with the cDNA increases the protein size around 8 kDa. (**B**) COS1 cells were transiently transfected with a plasmid encoding ephrin-B1 with that encoding flag-tagged CLD1 (lanes 1–4) or CLD4 (lanes 5–8). Cells were lysed and immunoprecipitated with an anti-flag (lanes 1, 5), mouse IgG1 (lanes 2, 6), anti-ephrin-B1 (C18 rabbit, lanes 3, 7) or normal rabbit serum (NRS) (lanes 4, 8). The precipitates were subjected to IB with anti-ephrin-B1 (C18 rabbit) or anti-claudin as indicated. The most upper band of co-precipitated ephrin-B1 at 48 kDa was partly overlapped with the band of immunoglobulin heavy chain (lane 5). The smaller-sized bands recognized with this antibody may be degradated products of ephrin-B1. (**C**) HT29 cells were lysed and immunoprecipitated (IP) with anti-ephrin-B1 (goat), anti-CLD1, anti-CLD4, NGS, and NRS or mouse IgG1, respectively, as indicated above the lanes. The precipitates were subjected to IB with anti-CLD1, anti-CLD4 or anti-ephrin-B1 (goat). Co-precipitated ephrin-B1 and claudins are indicated by arrowheads. (**D**) HT29 cells (left) or MDCK ephrin-B1 Tet-ON cells (right) were immunostained with the indicated antibodies. The corresponding computer-reconstructed vertical sections in the *X–Z* plane are shown.

 ©2005 European Molecular Biology Organization

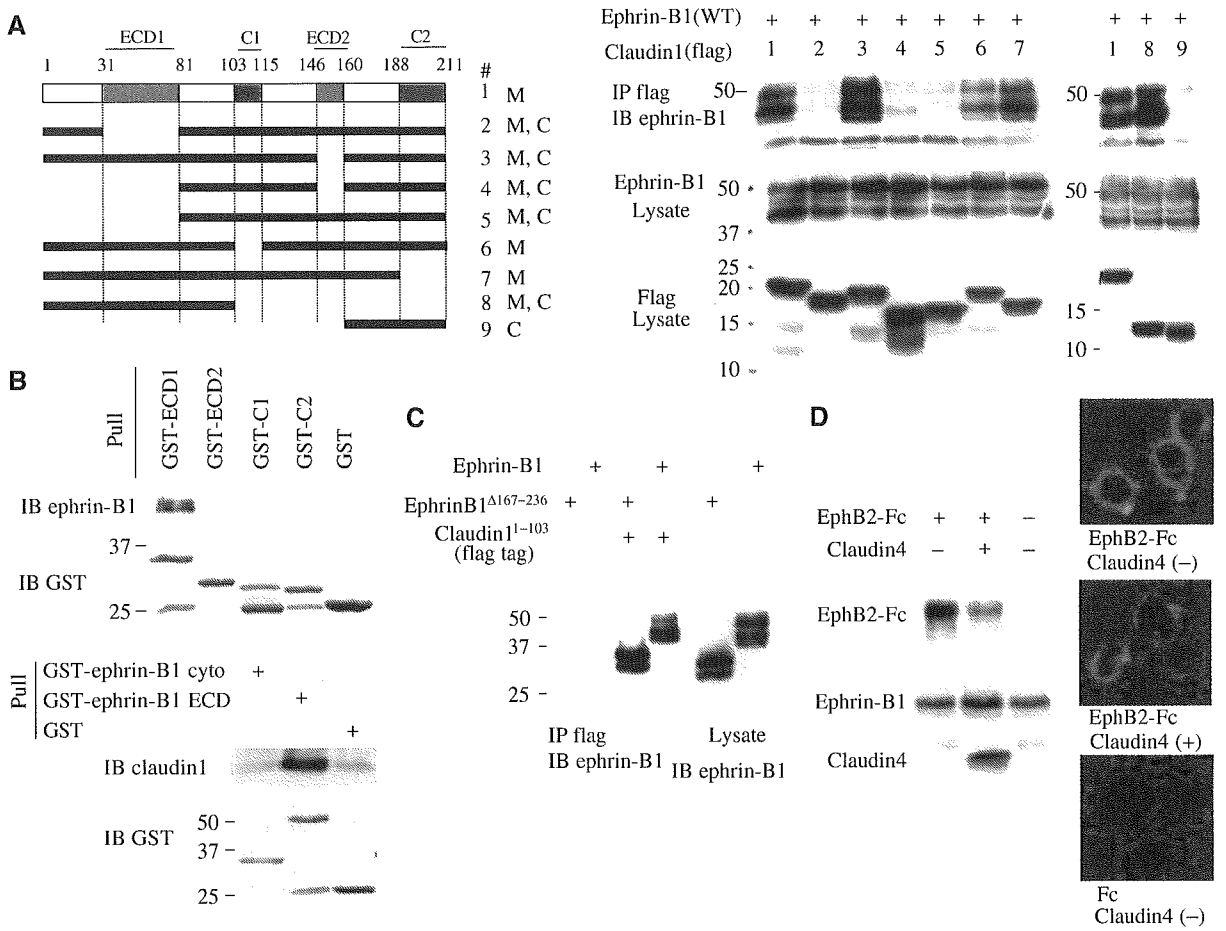

Figure 2 ECD of ephrin-B1 and claudins are required for their association: (**A**) A schematic diagram of the wild-type and deletion mutants of CLD1 used in this study. Proteins are depicted to scale: ECD1 and ECD2, the first and the second ECD; C1 and C2, the first and the second cytoplasmic domain. COS1 cells were transiently transfected with ephrin-B1, with flag-tagged deletion mutants of CLD1. The numbers indicated above the lanes correspond to those in the scheme. The cell lysates were immunoprecipitated (IP) with anti-flag and subjected to IB with anti ephrin-B1 (C18). The localization of each mutant in COS1 cells was examined by immunostaining, and depicted as M (cell membrane) and C (cytoplasm). The mutant #9 was mostly localized in the cytoplasm. (**B**) The lysates from COS1 cells transiently transfected with ephrin-B1 (top) or CLD1 (bottom) were incubated with GST-fusion protein of CLD1 or ephrin-B1 mutants described in Supplementary data 1. GST-fusion proteins were pulled with glutathione-sepharose beads, and the co-precipitated ephrin-B1 or CLD1 was detected by immunoblot. The input of GST-fusion proteins was shown by rehybridization of the filters with anti-GST antibody. The lower band at 25 kDa was observed in some GST-fusion proteins, which might be the degradated product. (**C**) COS1 cells were transiently transfected with flag-tagged $CLD1^{1-103}$ with a wild-type or deletion mutant of ephrin-B1. The cell lysates were immunoprecipitated with anti-flag and then immunoblotted with anti-ephrin-B1 (C18) antibody. (**D**) L ephrin-B1 were either infected with retrovirus containing recombinant CLD4 plasmid (CLD4 +) or mock plasmid (CLD4–), and treated with EphB2–Fc or control Fc at 10 μg/ml for 5 min as indicated. After washing, the cells were either lysed for subjecting to the IB with anti-mouse IgG to detect EphB2–Fc, or immunostained with anti-mouse Fc antibody and TOTO-3 iodide (left and right panels, respectively).

in Figure 2A), was not able to induce the phosphorylation of ephrin-B1 (Figure 3A, lane 3). Similarly, the corresponding mutant of CLD4 (CLD4 ΔECD1) did not affect the phosphorylation of ephrin-B1 (Figure 3A, lane 6). Moreover, the same result was also obtained using another cell line, HEK 293 cells (Figure 3B). The phosphorylation of ephrin-B1 through interaction with claudins was also confirmed by the reconstitution experiments using L cells, in which ephrin-B1 is endogenously expressed at a low level. The tyrosine phosphorylation of ephrin-B1 was clearly induced in L cells stably expressing CLD1 (L CLD1) or CLD4 (L CLD4) when compared to the parent L cells (Figure 3C). However, ephrin-B1 was not phosphorylated in L cells stably expressing claudins lacking in the first ECD (ΔECD1) or only the ECD1 of CLD1 or CLD4 (corresponding to #8 in Figure 2A). These results indicate that the association of claudin with ephrin-B1 is required for its phosphorylation, but the binding region located in the ECD1 of claudin was insufficient to induce the phosphorylation of ephrin-B1. The phosphorylation of ephrin-B1 by claudin took place on tyrosine residues in its cytoplasmic region, because the phosphorylation was almost completely abolished when four tyrosine residues within the cytoplasmic domain of ephrin-B1 were mutated (ephrin-B1 4YF; Figure 4A). Two tyrosine residues located at the carboxyl-terminus of ephrin-B1 (Tyr 343, 344) were not the major target of claudin-induced phosphorylation, because the phosphorylation level of ephrin-B1 remained almost unchanged following the mutation of these two tyrosines (data not shown).

We next examined whether the claudin-induced phosphorylation of ephrin-B1 was caused by Src family kinases (SFK), known to be responsible for the tyrosine phosphorylation of

©2005 European Molecular Biology Organization

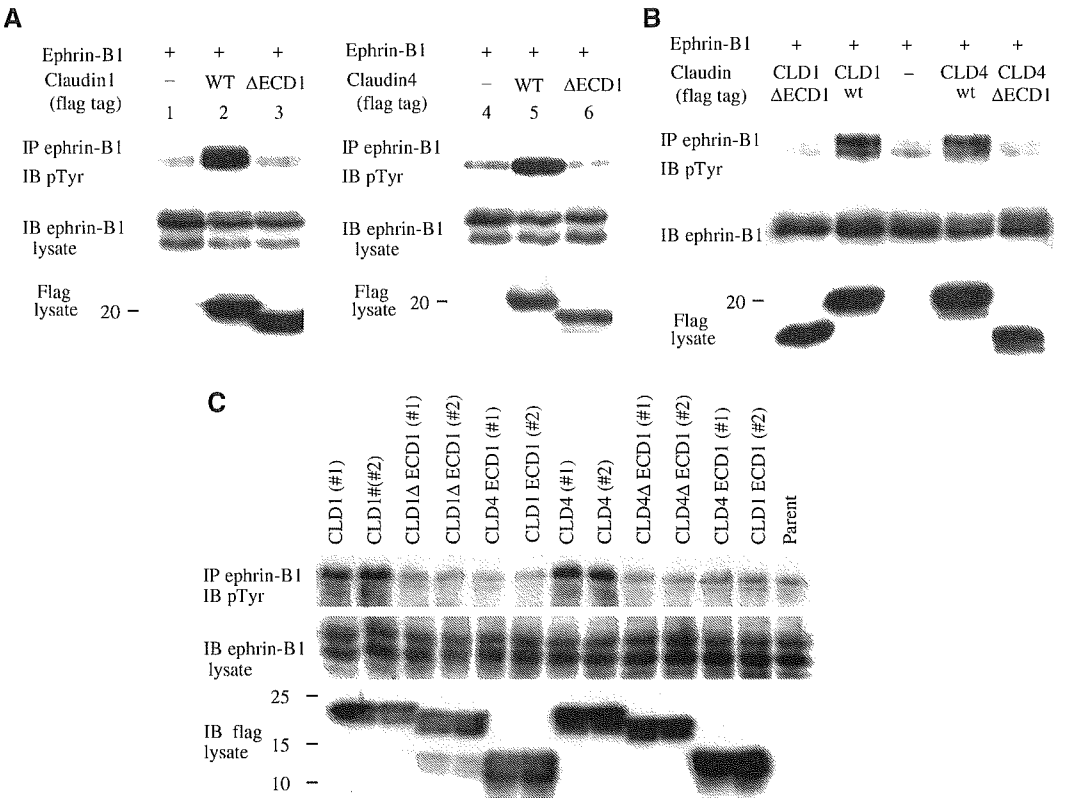

Figure 3 Ephrin-B1 is tyrosine phosphorylated by coexpression with claudins: (**A**) COS1 cells were transiently transfected with ephrin-B1 together with the wild type or mutant lacking the ΔECD1 of CLD1 (lanes 2, 3) or CLD4 (lanes 5, 6). Cell lysates were immunoprecipitated with anti-ephrin-B1 (goat) and subjected to IB with anti-phosphotyrosine (4G10). (**B**) HEK293 cells were transiently transfected with the plasmids as indicated. Cell lysates were subjected for the IP and IB as described in (A). (**C**) The cell lysates from either parent L cell, L cell lines stably expressing the wild type, ΔECD1 or the ECD1 of CLD1 or CLD4 were immunoprecipitated with anti-ephrin-B1 (goat) and subjected to IB with 4G10. Representative results of two independent clones (#1, 2) each are shown.

ephrin-B1 by the cognate Eph receptor stimulation. The treatment of the cells with 4-amino-5-(4-chlorophenyl)-7-(t-butyl)pyrazolo[3,4-d]pyrimidine (PP2), an inhibitor of the SFK, was seen to almost completely abolish the tyrosine phosphorylation of ephrin-B1 induced by the coexpression of CLD1 or CLD4 (Figure 4B). However, the control 4-amino-7-phenylpyrazol[3,4-d]pyrimidine (PP3) did not exhibit any effect on the tyrosine phosphorylation of ephrin-B1 in claudin-overexpressed cells (Figure 4B). Tyrosine phosphorylation of ephrin-B1 in stable lines of L CLD1 or L CLD4 was also inhibited by the treatment with PP2 (data not shown). These results suggest that ephrin-B1 is phosphorylated on tyrosine residues most probably via the activity of SFK following interaction with claudin. As interaction with EphB2 induces tyrosine phosphorylation of ephrin-B1, which in turn serves as the docking site for the Src homology 2 domain (SH2 domain) of Grb4 (Cowan and Henkemeyer, 2001), we examined whether claudin-induced phosphorylation of ephrin-B1 also induces association with Grb4. The GST fusion containing the SH2 domain of Grb4 was recruited to ephrin-B1 when ephrin-B1 was phosphorylated through coexpression with CLD1 or CLD4 (Supplementary data 2).

Phosphorylation of ephrin-B1 is significantly enhanced by cell–cell contact formation

The effect of cell–cell contacts on the phosphorylation of ephrin-B1 was then analyzed through the overlay coculture method using stable lines of L cells. L ephrin-B1 were overlaid on the parent cells or either CLD1- or CLD4-expressing cells, while, as a control, L ephrin-B1 cells were overlaid on the EphB2-expressing cells. Although ephrin-B1 was highly phosphorylated through the coculture with cells expressing EphB2, there was no significant phosphorylation of ephrin-B1 by the coculture with L CLD1 or L CLD4 (Supplementary data 3A). These results indicate that claudins do not stimulate the phosphorylation of ephrin-B1 through the mechanism of *trans*, intercellular association between the two proteins. On the other hand, ephrin-B1 was phosphorylated in L ephrin-B1 CLD1 when cocultured onto CLD1-expressing cells (Supplementary data 3B). Therefore, in response to the intercellular adhesion of claudins, ephrin-B1 may be phosphorylated through the interaction with adjacent claudins in the same cell membrane. We then tested the possibility of ephrin-B1 interacting with claudin *in cis* on the same cells. In L CLD4, ephrin-B1 associated with CLD4 even when they were plated as scattered single cells (Figure 5A, lane 4). The tyrosine phosphorylation of ephrin-B1 was seen to be greatly influenced by the cell density. Ephrin-B1 was highly phosphorylated when L CLD4 were plated at a high density, while it was reduced when the cells were plated as scattered single cells (Figure 5A, comparing lanes 4 and 6). On the other hand, the phosphorylation level of ephrin-B1 in the parent L cells was low and apparently unchanged by the cell density (Figure 5A, bottom, right). In order to examine the

 ©2005 European Molecular Biology Organization

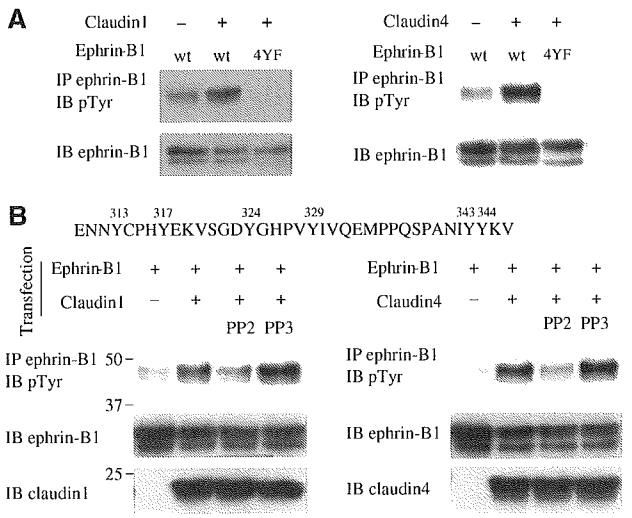

Figure 4 PP2 inhibits the phosphorylation of ephrin-B1 induced by claudins. (**A**) COS1 cells were transfected with the indicated plasmids. In (**B**), transfected cells were treated with PP2 or PP3 as described in Materials and methods. Ephrin-B1 was immunoprecipitated from individual cell lysate, and subjected to IB with 4G10. The amino-acid sequence of the carboxyl-tail of human ephrin-B1 is shown at the bottom of (A). The cell lysates were immunoblotted with anti-ephrin-B1 (goat) or anti-claudin antibodies to detect the expression level (bottom).

effect of the claudin–claudin *trans* adhesion accompanied by the cellular contact on the phosphorylation of ephrin-B1, the phosphorylation level of ephrin-B1 was evaluated during the dynamic change of the intercellular adhesion. When cell–cell interaction was completely disrupted by the depletion of calcium in the medium, the tyrosine phosphorylation of ephrin-B1 was also abolished (Figure 5B). Similar results were obtained in L CLD1 (data not shown). On the other hand, the cell dissociation did not modify the phosphorylation level of ephrin-B1 in the parent L cells (Figure 5B, bottom). In order to exclude the possibility that intracellular concentration of calcium may also have been decreased by the cell incubation with ethylene glycol bis (β-aminoethyl ether) *N,N,N′,N′*-tetraacetic acid (EGTA) and have affected the phosphorylation of ephrin-B1, we performed a control experiment where cells were treated with nifedipine, a blocker of the calcium channel. The decrease in the level of intracellular calcium caused by nifedipine did not affect the status of the association of ephrin-B1 with claudin, nor the phosphorylation of ephrin-B1 (data not shown). Therefore, these results suggest that the phosphorylation of ephrin-B1 through the interaction of claudin was significantly induced by cell–cell contact.

The previous conclusion was further supported by the examination of the intracellular localization of tyrosine-

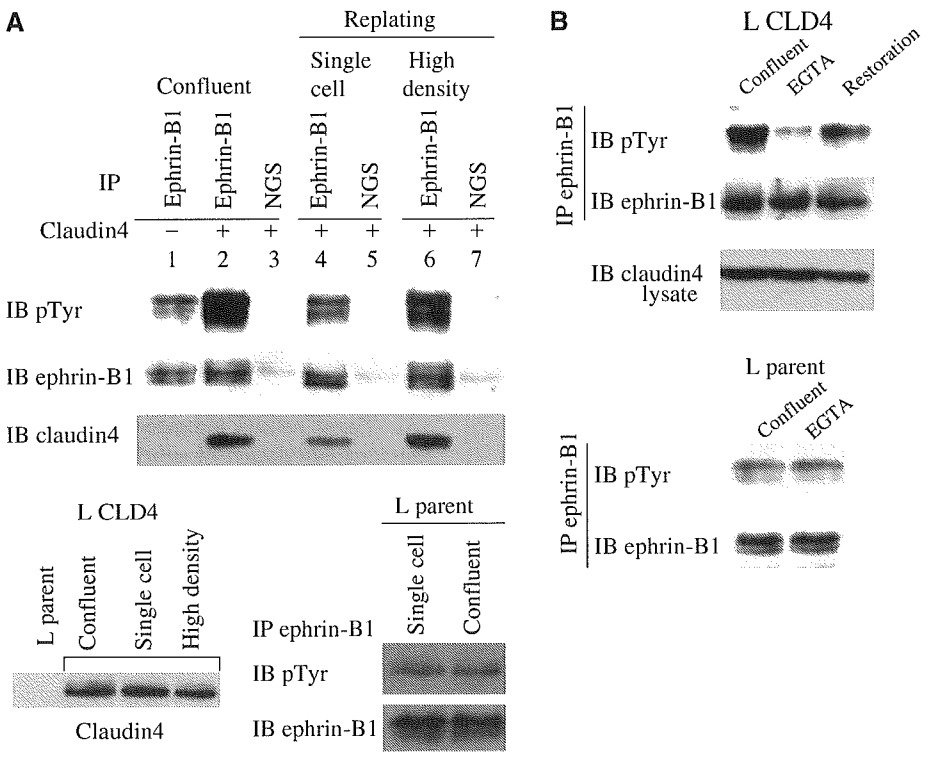

Figure 5 The phosphorylation of ephrin-B1 correlates with the cell–cell interactions. (**A**) Parent L cells (lane 1) or L cells stably expressing CLD4 (L CLD4, lanes 2–7), which were indicated as CLD4 (–) or (+) above the lanes, were grown until confluent. The cells were detached by EGTA, and replated on new dishes either at a low density as scattered single cells or at a high density. Cells were lysed for IP with anti-ephrin-B1 or NGS) which were then subject to IB with 4G10 (pTyr). The membrane was re-hybridized with anti-ephrin-B1 (goat) or anti-CLD4 antibody. The expression of CLD4 in each cell lysate was confirmed by IB (bottom, left). Bottom, right: The tyrosine phosphorylation of ephrin-B1 in parent L cells was examined when the cells were plated as single cells or at a high cell density. (**B**) L CLD4 (top) or parent L cells (bottom) were grown until confluent. The cells were incubated in HBSS$^-$ containing 2 mM EGTA until the majority of the cell–cell contacts were lost, but not detached from the substrate. After washing, monolayers were incubated in the cell culture medium for 4 h. The cells were lysed before (confluent) and after calcium depletion (EGTA), and after changing to the normal cell culture medium for 4 h (restoration) to analyze the phosphorylation of ephrin-B1 as described in (A).

©2005 European Molecular Biology Organization

phosphorylated ephrin-B1, with the phospho-specific antibody generated against Tyr317 of ephrin-B1. Tyr317 of ephrin-B1 (corresponding to Tyr305 of mouse ephrin-B1) is phosphorylated when stimulated with EphB2, and is a critical requirement for interaction with Grb4 (Bong *et al*, 2004). In the L ephrin-B1, tyrosine phosphorylation of ephrin-B1 was not observed, regardless of the cell density involved (Figure 6, columns A and C). On the other hand, the L ephrin-B1 CLD1 showed the tyrosine phosphorylation of ephrin-B1 clearly at the cell–cell contact sites, although it was not detected in single isolated cells (Figure 6, columns B and D). The same results were obtained when L CLD4 were used (data not shown), while these observations were further supported by the same analysis using MDCK ephrin-B1 Tet-ON cells, where CLD1 and CLD4 were endogenously expressed (Supplementary data 4).

In the L and MDCK cell lines used in this study, there was no detectable expression of EphB2 exposed through immunoblot analysis (data not shown). The enhancement of the tyrosine phosphorylation of EphB2 was not detected after these cells were treated with ephrin-B1–Fc (Supplementary data 5A). Moreover, when L or MDCK cells were incubated with ephrin-B1–Fc, the membrane-bound ephrin-B1–Fc was not detected following staining with anti-Fc antibody (Supplementary data 5B). The treatment of the cells with an excess volume of soluble ephrin-B1 blocks receptors to interact with membrane-bound ephrin-B1 *in trans*, thereby shutting off the reverse signaling. On the other hand, the ephrin-B1 phosphorylation level was not attenuated in the L and MDCK cell lines through the addition of ephrin-B1–Fc (Supplementary data 5C), indicating that receptors stimulating ephrin-B1 are not detected in these cells.

Phosphorylation of ephrin-B1 is enhanced by ECD of CLD1

In order to evaluate the possibility that claudin–claudin *trans* interaction enhances the tyrosine phosphorylation of ephrin-B1, CLD1–Fc fusion protein was prepared. For mimicking the *trans* interaction between claudins mediated by the intercell contacts, the first and the second ECDs of CLD1, which were linked by flag-epitope tag, were fused to the Fc region of immunoglobulin. Preclustered CLD1–Fc attached to HT29 cell membrane, and at least a part of CLD1 in the cell membrane was colocalized with the CLD1–Fc (Figure 7A). Moreover, the endogenous CLD1 protein was co-precipitated with CLD1–Fc (Figure 7B, top). These results indicate that the CLD1–Fc fusion protein effectively binds to the cellular CLD1 at the cell surface. The induction of ephrin-B1 phosphorylation was not evident by adding the preclustered soluble CLD1–Fc in the culture medium of L ephrin-B1 CLD1 (data not shown). On the other hand, when the cells were plated on preclustered CLD1–Fc-coated plates, ephrin-B1 was phosphorylated on tyrosine residues (Figure 7B, bottom). Although the enhanced phosphorylation of ephrin-B1 was detected within 30 min after the cells were attached on the CLD1–Fc precoated plates (data not shown), we noticed faster attachment of CLD1-expressing L cells on CLD1–Fc-coated plate compared to that on albumin-coated plate. On the other hand, no significant difference was observed in cell attachment and spreading between these two plates at 3 h after plating, when our biochemical analyses were performed. To further confirm this result, we examined the induction of ephrin-B1 phosphorylation using CLD1–Fc-coated microbeads. When clustered CLD1–Fc beads were added on L ephrin-B1 CLD1, phosphorylation of ephrin-B1

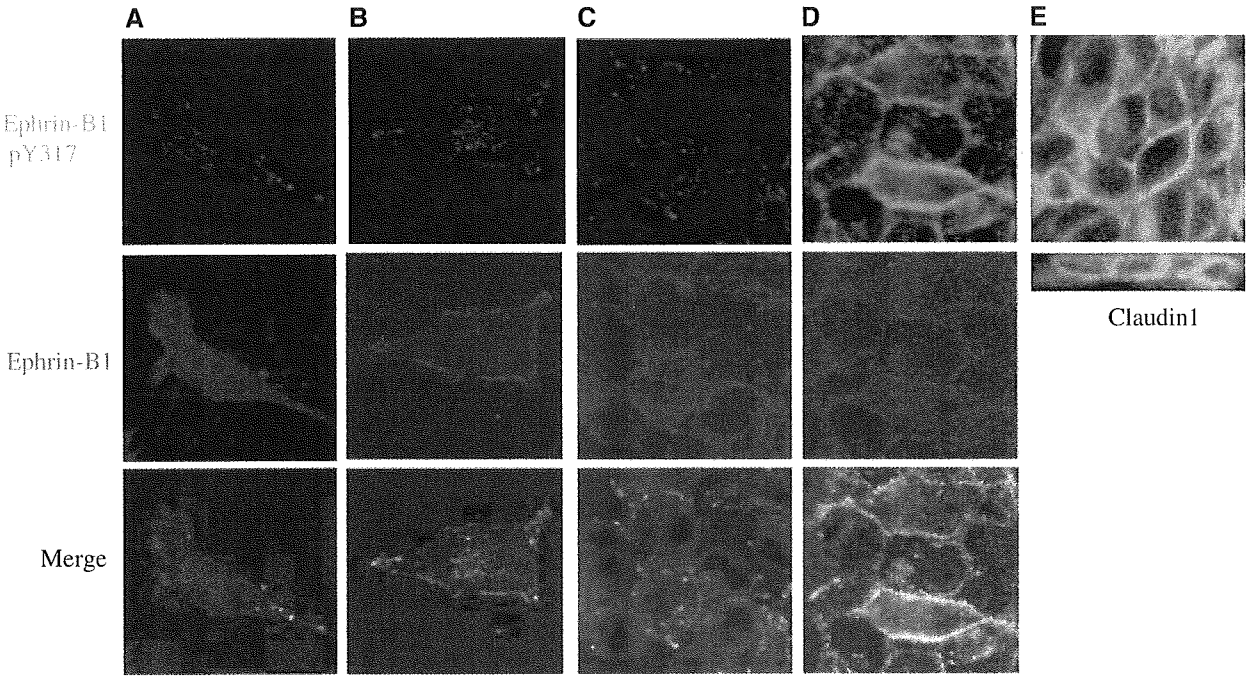

Figure 6 The intercellular interaction of L CLD induced tyrosine phosphorylation of ephrin-B1. (**A–D**) L ephrin-B1 (columns A, C) or L ephrin-B1 CLD1 (columns B, D) were plated either at a low (columns A, B) or high (columns C, D) cell density. The cells were immunostained with anti-ephrin-B1 (red) and anti-pTyr ephrin-B1 (green) antibodies while the nucleus was stained with TOTO-3 iodide. (**E**) The expression of cludin1 in L ephrin-B1 CLD1 cells is shown.

©2005 European Molecular Biology Organization

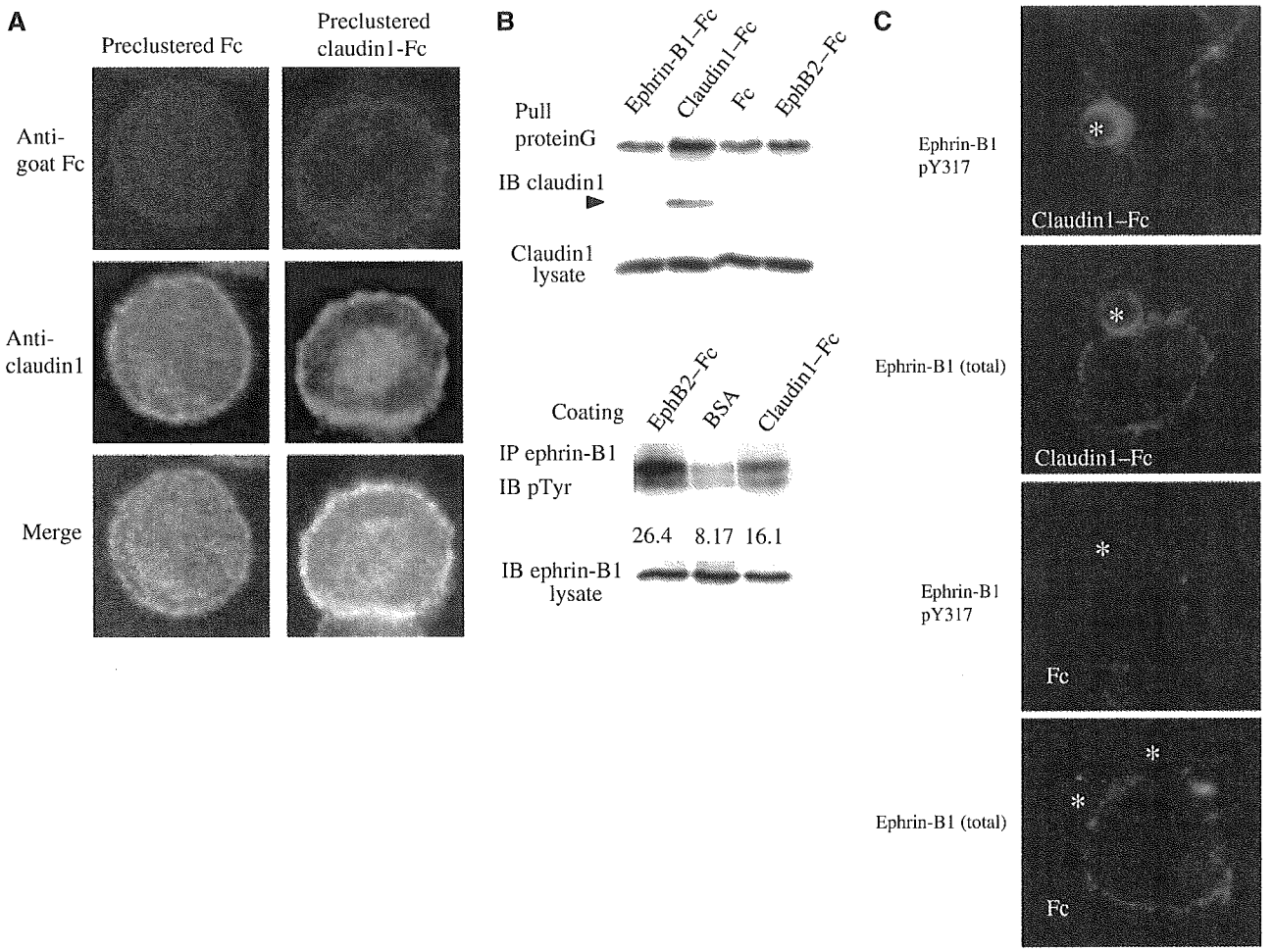

Figure 7 Clustered extracellular domains of claudin stimulate the phosphorylation of ephrin-B1. (**A**) HT29 cells were incubated with preclustered CLD1–Fc or the control Fc at 2 μg/ml for 1 h. The cells were immunostained with anti-CLD1 (green) and anti-Fc antibody (red). (**B**) Top: L CLD1 were incubated with Fc-fusion proteins as indicated. The cell lysates were precipitated with protein-G Sepharose, and subjected to IB with anti-CLD1 antibody. Bottom: L ephrin-B1 CLD1 were seeded at a low cell density on the plates coated with EphB2–Fc, BSA, or CLD1–Fc, as described in Materials and Methods. Ephrin-B1 was immunoprecipitated from the cell lysates 3 h after plating, and subjected to IB with 4G10. Values below each band are relative density of the bands. The same filter was re-hybridized with anti-ephrin-B1 antibody. (**C**) Microbeads precoated with claudin–Fc or control Fc were added to L ephrin-B1 CLD1. After 30 min incubation, cells were fixed, and immunostained with anti-pTyr ephrin-B1 or anti-ephrin-B1 (C18) antibody, which reacts with the C-terminal region of ephrin-B1 together with TOTO-3 iodide. The positions of the beads were marked with asterisks.

was detected on cell membrane contacting to the bead (Figure 7C). Moreover, ephrin-B1 was concentrated at the bead–cell contact sites (Figure 7C). On the other hand, we could not detect either phosphorylation or concentration of ephrin-B1 at the contact sites to the control Fc-coated beads.

Tyrosine phosphorylation of ephrin-B1 affects cell–cell adhesion

In order to understand the biological effects of the interaction of ephrin-B1 with claudins, we examined its potential influence on cell–cell adhesion. No significant morphological change in the confluent MDCK cells was observed even when ephrin-B1 expression was induced by doxycycline (Figure 8A, 'No Treatment'). On the other hand, apparent delay in the restoration of the cell–cell adhesion after calcium switch (see Materials and methods) was observed by inducible expression of ephrin-B1 (Figure 8A). To quantify this morphological observation, paracellular flux of fluorescence-labeled dextran was monitored in MDCK cells. The decrease in paracellular flux after calcium switch was also delayed in cells overexpressing ephrin-B1 (Figure 8B).

The effects of various ephrin-B1 mutants on cell adhesion were next compared by expressing wild type or mutants of ephrin-B1 through adenovirus-mediated gene transfer in confluent MDCK cells. Expression of wild-type ephrin-B1 slightly increased the permeability compared to expression of control GFP (Figure 8C, top). The difference was enhanced when the permeability was measured periodically during the weak treatment of the cells with calcium-chelating agent under the condition that phosphorylation of wild-type ephrin-B1 was still maintained (Figure 8C, bottom). On the other hand, the expression of ephrin-B1 lacking the cytoplasmic region (Δcyto) and the ephrin-B1 with the mutation of tyrosine residues in the cytoplasmic region (4YF) did not greatly affect the paracellular permeability (Figure 8C). In contrast, the expression of ephrin-B1 mutant lacking the valine at the carboxyl-tail (ΔV), which is reported to be critical for binding PDZ domain-containing proteins,

©2005 European Molecular Biology Organization

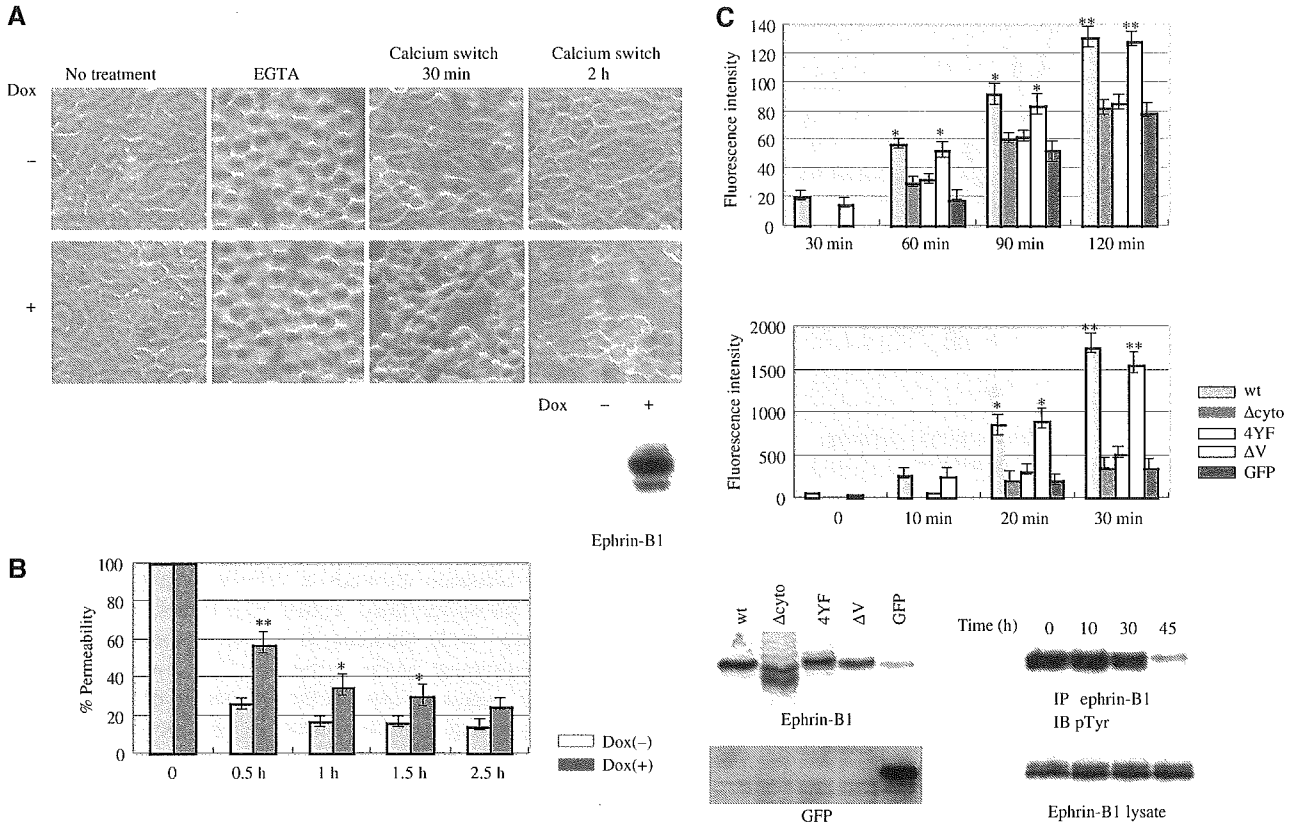

Figure 8 Tyrosine phosphorylation of ephrin-B1 affects intercellular adhesion: (**A**) MDCK ephrin-B1 Tet-ON cells were grown on culture dishes until confluent with (+) or without (−) the addition of doxycycline (Dox). The cells were incubated in HBSS⁻-containing EGTA. The medium was then replaced by one containing calcium (calcium switch), and the cells were incubated for the indicated period. (**B**) MDCK ephrin-B1 Tet-ON cells grown in the Transwell chambers (Dox− or Dox+) were treated with EGTA to increase the initial permeability to almost the same levels. The monolayers were allowed to recover in the calcium-containing medium for the indicated period, then subject to FITC-dextran flux measurement. The results are presented in terms of the % fluorescence of the cells without recovery. Each bar represents the mean values ± s.d. from four independent experiments, each in duplicate. The asterisk indicates differences from Dox (−) cells at each time point. $^{*}P<0.05$, $^{**}P<0.01$. (**C**) Confluent MDCK cells grown in Transwells were infected with Ad-ephrin-B1, Ad-Δcyto ephrin-B1, Ad-4YF ephrin-B1, Ad- ΔV ephrin-B1 or Ad-GFP as described in Materials and methods. Top: The FITC-dextran flux during the indicated time was measured without pretreatment of EGTA. Bottom: The infected cells were treated with EGTA for the indicated period, and then FITC-dextran flux during the next 30 min was measured. This experiment was performed under the conditions of cell–cell contact remaining after treatment with EGTA, which was confirmed through the microscopic observation. Expression of ephrin-B1 from each construct in infected MDCK cells and the phosphorylation level of ephrin-B1 at each time point of EGTA treatment were shown at the bottom (left and right panels, respectively). The results from four independent experiments, each in duplicate, are shown as the mean values ± s.d. The asterisk indicates differences from the permeability of GFP-infected cells at each time point. $^{*}P<0.01$, $^{**}P<0.001$.

increased the permeability as well as wild-type ephrin-B1, suggesting that this residue is not crucial for the regulation of cell–cell adhesion. These results suggest that ephrin-B1 affects cell–cell adhesion depending on its tyrosine phosphorylation.

Discussion

Examination of the mode of association between claudin andephrin-B1 revealed that claudin associates with ephrin-B1 on the same cell surface. The formation of cell–cell contact remarkably enhances the phosphorylation of ephrin-B1 in a claudin-dependent manner. Our result further suggests that claudin–ephrin-B1 complex attenuates cell–cell adhesion through the phosphorylated cytoplasmic domain of ephrin-B1 (Figure 9). The association of ephrin-B1 with CLD1 and CLD4 was detected in the single cells. On the other hand, ephrin-B1–Fc did not bind to the CLD1 expressed on the cell membrane (Figure 7B), and, similarly, CLD1–Fc in the culture medium did not bind to ephrin-B1 (data not shown). Together with the observation that claudins did not stimulate the phosphorylation of ephrin-B1 in opposing membrane through the overlay coculture method (Supplementary data 3A), these results suggest that ephrin-B1 and claudins associate *in cis* on the same cell membrane, but not *in trans*.

In order to propose the novel mechanism for the activation of ephrin-B1 reverse signaling though claudins, we showed the ephrin-B1 phosphorylation in several cell lines in which the effects of cognate receptor EphB appear to be little or negligible. In COS1 cells, which were used to show the effect of claudin ECD1 on the phosphorylation of ephrin-B1, very little amount of EphB2 receptor was detected (Supplementary data 5A), there remaining a slight possibility that this receptor affects the phosphorylation state of ephrin-B1. Actually, there is a possibility that overexpressed claudin enhanced cell–cell interaction, which resulted in increased EphB2–ephrin-B1 interactions and enhanced ephrin-B1 phosphorylation. Therefore, HEK 293 cell, which according to several

 ©2005 European Molecular Biology Organization

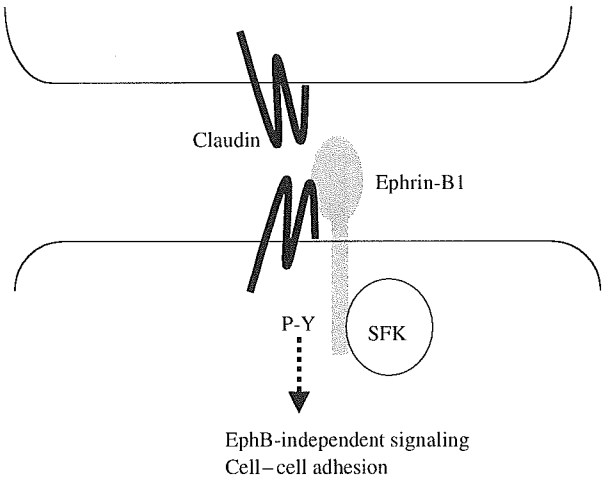

Figure 9 Diagram showing the possible relation between ephrin-B1 and claudin. The intercellular interaction of claudins stimulates the tyrosine phosphorylation of ephrin-B1 most probably through the activation of SFK, which may transduce signaling to the downstream effectors. The phosphorylation of ephrin-B1 directly or indirectly modifies the degree of cell–cell adhesion.

reports do not contain detectable levels of Eph receptors that bind ephrin-B1, was also used to confirm the results (Figure 3B) (Zisch *et al*, 2000; Miao *et al*, 2005).

The cognate receptors for ephrin-B1 were not detected in L cells and MDCK cells by ephrin-B1–Fc labeling (Supplementary data 5B), and at least EphB1, EphB2 and EphB3 were not detected by RT–PCR in L cells (data not shown). Moreover, ephrin-B1 phosphorylation level was not attenuated by the addition of soluble ephrin-B1 in L and MDCK cells (Supplementary data 5C), which was consistent with the observation that soluble ephrin-B1 blocks the EphB receptor-stimulated signaling, but does not affect the interaction between ephrin-B1 and claudin on the same cell membrane. Together with the observation that immobilized CLD1–Fc directly phosphorylated ephrin-B1, these results suggest that ephrin-B1 phosphorylation was enhanced by the interaction with claudins.

The phosphorylation of ephrin-B1 in claudin-expressing L cells was markedly increased in the existence of cell–cell adhesion. Although we cannot rule out the possibility that less amount of association between ephrin-B1 and claudin in single scattered cells may affect the phosphorylation level of ephrin-B1 (Figure 5A), clustered CLD1–Fc fusion protein coated on the plates or microbeads enhanced ephrin-B1 phosphorylation, suggesting that the intercellular interaction of claudins is most probably required for the phosphorylation of ephrin-B1. This increase in tyrosine phosphorylation cannot be explained by any other adhesion molecules or any cognate receptor for ephrin-B1, since the phosphorylation level of ephrin-B1 in parent L cells did not alter according to cell density (Figure 5). The fact that the incubation of the cells with soluble clustered CLD1–Fc was not as effective for the phosphorylation of ephrin-B1, suggests a functional difference between soluble clustered claudin and the endogenous claudin on the cell membrane. It is well known that the clustering of ephrin-B1 on the cell membrane represented the trigger of its phosphorylation when stimulated by the EphB2–Fc fusion protein. The intercellular interaction of claudins may enhance the local concentration of associating ephrin-B1, resulting in oligomerization and the activation of ephrin-B1 as a substrate of SFK. As the isolated ECD1 of CLD1 or CLD4 could not activate tyrosine phosphorylation of ephrin-B1, such concentration of ephrin-B1 may not be induced by the isolated ECD1 of claudins. Alternatively, the intercellular interaction of claudins may directly stimulate the activation of SFK, which in turn phosphorylate ephrin-B1 associating with the claudin. However, the presence of such activation of the SFK in response to the intercellular interaction of claudins is as yet unknown. In addition, the cause of the basal level of ephrin-B1 phosphorylation in parent L cells is not still clear. There still remains the possibility that some other mechanism causing the slight phosphorylation of ephrin-B1.

Ephrin-B1 increased the degree of paracellular permeability, which is a consequence of the tyrosine phosphorylation of the cytoplasmic domain of ephrin-B1. This result suggests that the interaction of claudins with ephrin-B1 attenuated cell–cell adhesion through a cellular signal transduction through phosphorylated ephrin-B1, rather than physical interference with claudins to make homophilic clusters. The measurement of the permeability of low-molecular-size dextran is commonly used for the assessment of tight junctions. However, phosphorylated ephrin-B1 does not seem to exclusively modify the function of tight junctions, because it affected the gross change of cell–cell adhesion. Although the phosphorylation of ephrin-B1 was induced by claudins, further precise examination is necessary to determine which adhesion molecule is the primary target of phosphorylated ephrin-B1. The ephrin-B1 phosphorylation does not regulate cell–cell adhesion through the modification of the expression levels of the proteins composing tight or adherence junctions. For example, the overexpression of ephrin-B1 in MDCK cells induced by doxycyline did not change the protein expression levels of CLD1, CLD4, ZO-1, E-cadherin and β-catenin (data not shown).

The expression of ephrin-B1 increased the permeability during both the processes of destabilizing the cell adhesion through EGTA treatment and restoring cell–cell adhesion after the calcium switch. The intracellular localization of claudins may therefore be important for the ephrin-B1-mediated regulation of cell–cell adhesion. When claudins are localized to tight junctions in a restrictive manner, ephrin-B1 may not be phosphorylated widely. In our assay of paracellular flux, overexpression of ephrin-B1 was induced in MDCK cells by adenovirus infection after the cells reached confluent, which might be the reason why ephrin-B1 did not increase the permeability effectively without treatment of the calcium-chelating agent. The disruption of tight junctions through calcium depletion leads to the presence of naive cell–cell contacts with the diffusion of claudins on the cell membrane, which may further stimulate ephrin-B1 phosphorylation more widely, and accelerate the cell dissociation. The intercellular interaction between claudins occurs also in naive-contact cells, which do not possess the mature tight junction strands. In the calcium-switching process, the formation of new cell–cell contact triggers the ephrin-B1 phosphorylation, which may then delay the construction of the firm cell–cell adhesion. Such mechanisms may be also involved in the event of epithelial-to-mesenchymal transition during the invasion and metastasis of some carcinoma cells. Alternately,

©2005 European Molecular Biology Organization

ephrin-B1-expressing MDCK cells may be settled in a 'ready to dissociate' state when they are confluent. Upon the depletion of the extracellular calcium, the breaking up of cell–cell adhesion structures might be accelerated in these cells. The morphological observation of ephrin-B1-expressing MDCK cells (Figure 8A) also suggests that the phosphorylation of ephrin-B1 may affect the spreading of the cells resulting from the modification of cell-to-substrate adhesion.

Recent studies show that cell adhesion can trigger ligand-independent activation of growth factor receptors (Comoglio *et al*, 2003). For example, EGF receptor associates with E-cadherin. Following the cell–cell contact formation, an EGF receptor was found to be phosphorylated on tyrosine residues, which in turn activated MAP kinase and Rac in the absence of EGF stimulation (Pece and Gutkind, 2000; Betson *et al*, 2002). Claudins may play roles in translating environmental cues into intracellular signals through coupling with ephrin-B1 according to our results. Some of the claudins are frequently overexpressed in many cancer cells from the studies involving screening of the genes preferentially expressed in malignant cells. Therefore, claudins may play significant roles in carcinogenesis or the progression of cancers. In HT29 colon cancer cells, ephrin-B1 and claudins were found to be diffusely localized on the cell membrane, which may increase the chance of inducing ephrin-B1 phosphorylation. Novel signaling through the interaction of ephrin-B1 with claudins may inhibit the formation of tight adhesive structures during the process of cell–cell contact in some carcinoma cells, which may, in turn, affect malignant phenotypes such as invasion and metastasis of the carcinomas.

Materials and methods

Plasmids and antibodies, cDNA library, cell culture, IP and cell staining

Plasmids and antibodies used in this study and the methods of the library screening, cell culture, IP and cell staining are described in Supplementary data 1.

Preparation of CLD1–Fc-coated beads

Latex-sulfate microspheres (5.2 μm diameter; Interfacial Dynamics Corporation) were coated with CLD1–Fc fusion protein as reported (Honda *et al*, 2003). Briefly, beads were suspended in 0.1 M borate buffer, pH 8.0, and incubated with goat anti-mouse IgG (Fc-specific) antibody (ICN). After the beads were washed with PBS, the beads were then incubated with CLD1–Fc protein. After the incubation, the beads were washed three times with PBS, and resuspended in PBS containing 5 mg/ml bovine serum albumin (BSA).

Generation of adenoviruses and adenoviral infection

To generate recombinant adenoviruses, cDNAs encoding wild type or various mutants of ephrin-B1 were subcloned into the vector pShuttle-CMV (Stratagene). Transposition of the ephrin-B1 cDNAs from the pShuttle-CMV into pADEasy-1 (Stratagene) created the adenoviral vectors pAD-ephrin-B1 (wild type, Δcyto, 4YF, ΔV), where the transgenes were under the control of a CMV promoter. Recombinant adenoviral DNA was transfected into 293 human embryonic kidney cells to allow the production of adenoviral particles. The titer of adenovirus stocks was determined by an Adeno-X rapid titer kit (Clontech). Confluent MDCK cells grown on Transwell filters or glass coverslips were infected with adenoviruses at a multiplicity of infection (MOI) of 5 in medium containing 10% FBS. Following incubation for 12 h, the virus-containing medium was removed and fresh medium containing 10% FBS was added. The infected cells were used for the permeability assay 48 h after the infection.

Paracellular permeability assay

MDCK cells were grown until confluent in Transwell chambers, then the cells were either left untreated or treated with doxycycline (2 μg/ml) for 48 h prior to subject to the assay. In some experiments, the medium of both the upper and lower wells was replaced with Hank's balanced salt solutions ($HBSS^-$) containing 2 mM of EGTA for the indicated period. We performed the experiments under the conditions of cell–cell contact remaining after treatment with EGTA, which was confirmed through the microscopic observation. In some experiments, the monolayers were allowed to recover in the calcium-containing medium (calcium switch) with 0.5% FBS for the indicated period. Then, the upper well was replaced to the normal medium containing 0.5% FBS with FITC-dextran (MW 3000) at a concentration of 10 μg/ml. Following incubation for the indicated period, samples were taken from the lower compartment of the Transwell chambers. The amount of FITC-dextran in the lower wells was measured using Beacon 2000 (Takara), with an excitation wavelength of 490 nm and detection of emissions at 530 nm. Student's *t*-test was used to analyze data from four independent experiments, each in duplicate.

Supplementary data

Supplementary data are available at *The EMBO Journal* Online.

Acknowledgements

We thank Dr S Tsukita (Kyoto University) for providing the plasmids used in this study. This study was supported by the Program for the Promotion of Fundamental Studies in Health Science of the Organization for Pharmaceutical Safety and Research of Japan.

References

Batlle E, Henderson JT, Beghtel H, Van den Born MM, Sancho E, Huls G, Meeldijk J, Robertson J, Van de Wetering M, Pawson T, Clevers H (2002) β-catenin and TCF mediate cell positioning in the intestinal epithelium by controlling the expression of EphB/Ephrin-B. *Cell* **111**: 251–263

Betson M, Lozano E, Zhang J, Braga VM (2002) Rac activation upon cell–cell contact formation is dependent on signaling from the epidermal growth factor receptor. *J Biol Chem* **277**: 36962–36969

Bong YS, Park YH, Lee HS, Mood K, Ishimura A, Daar IO (2004) Tyr-298 in ephrinB1 is critical for an interaction with the Grb4 adaptor protein. *Biochem J* **377**: 499–507

Brantley-Sieders D, Parker M, Chen J (2004) Eph receptor tyrosine kinases in tumor and tumor microenvironment. *Curr Pharm Des* **10**: 3431–3442

Bruckner K, Pasquale EB, Klein R (1997) Tyrosine phosphorylation of transmembrane ligands for Eph receptors. *Science* **275**: 1640–1643

Comoglio PM, Boccaccio C, Trusolino L (2003) Interactions between growth factor receptors and adhesion molecules: breaking the rules. *Curr Opin Cell Biol* **15**: 565–571

Cowan CA, Henkemeyer M (2001) The SH2/SH3 adaptor Grb4 transduces B-ephrin reverse signals. *Nature* **413**: 174–179

Fujita M, Itoh M, Shibata M, Taira S, Taira M (2002) Gene expression pattern analysis of the tight junction protein, Claudin, in the early morphogenesis of *Xenopus* embryos. *Mech Dev* **119**: S27–S30

Furuse M, Sasaki H, Fujimoto K, Tsukita S (1998) A single gene product, claudin -1 or -2, reconstitutes tight junction strands and recruits occludin in fibroblasts. *J Cell Biol* **143**: 391–401

Himanen JP, Rajashankar KR, Lackmann M, Cowan CA, Henkemeyer M, Nikolov DB (2001) Crystal structure of an Eph receptor–ephrin complex. *Nature* **414**: 933–938

Holland SJ, Gale NW, Mbamalu G, Yancopoulos GD, Henkemeyer M, Pawson T (1996) Bidirectional signalling through the EPH-

©2005 European Molecular Biology Organization

family receptor Nuk and its transmembrane ligands. *Nature* **383**: 722–725

Honda T, Shimizu K, Kawakatsu T, Yasumi M, Shingai T, Fukuhara A, Ozaki-Kuroda K, Irie K, Nakanishi H, Takai Y (2003) Antagonistic and agonistic effects of an extracellular fragment of nectin on formation of E-cadherin-based cell–cell adhesion. *Genes Cells* **8**: 51–63

Jones TL, Chong LD, Kim J, Xu RH, Kung HF, Daar IO (1998) Loss of cell adhesion in *Xenopus laevis* embryos mediated by the cytoplasmic domain of XLerk, an erythropoietin-producing hepatocellular ligand. *Proc Natl Acad Sci USA* **95**: 576–581

Kullander K, Klein R (2002) Mechanisms and functions of Eph and ephrin signalling. *Mol Cell Biol* **3**: 475–486

Lin D, Gish GD, Songyang Z, Pawson T (1999) The carboxyl terminus of B class ephrins constitutes a PDZ domain binding motif. *J Biol Chem* **274**: 3726–3733

Lu Q, Sun EE, Klein R, Flanagan JG (2001) Ephrin-B reverse signaling is mediated by a novel PDZ-RGS protein and selectively inhibits G-protein coupled chemoattraction. *Cell* **105**: 69–79

Miao H, Strebhardt K, Pasquale EB, Shen TL, Guan JL, Wang B (2005) Inhibition of integrin-mediated cell adhesion but not directional cell migration requires catalytic activity of EphB3 receptor tyrosine kinase. *J Biol Chem* **280**: 923–932

Morita K, Furuse M, Fujimoto K, Tsukita S (1999) Claudin multigene family encoding four-transmembrane domain protein components of tight junction strands. *Proc Natl Acad Sci USA* **96**: 511–516

Murai KK, Pasquale EB (2003) Ephective signaling: forward, reverse and crosstalk. *J Cell Sci* **116**: 2823–2832

Palmer A, Zimmer M, Erdmann KS, Eulenburg V, Porthin A, Heumann R, Deutsch U, Klein R (2002) Ephrin-B phosphorylation and reverse signaling: regulation by Src kinases and PTP-BL phosphatase. *Mol Cell* **9**: 725–737

Pece S, Gutkind JS (2000) Signaling from E-cadherins to the MAPK pathway by the recruitment and activation of epidermal growth factor receptors upon cell–cell contact formation. *J Biol Chem* **275**: 41227–41233

Poliakov A, Cotrina M, Wilkinson DG (2004) Diverse roles of Eph receptors and ephrins in the regulation of cell migration and tissue assembly. *Dev Cell* **7**: 465–480

Surawska H, Ma PC, Salgia R (2004) The role of ephrins and Eph receptors in cancer. *Cytokine Growth Factor Rev* **15**: 419–433

Torres R, Firestein BL, Dong H, Staudinger J, Olson EN, Huganir RL, Bredt DS, Gale NW, Yancopoulos GD (1998) PDZ proteins bind, cluster, and synaptically colocalize with Eph receptors and their ephrin ligands. *Neuron* **21**: 1453–1463

Tsukita S, Furuse M, Itoh M (2001) Multifunctional strands in tight junctions. *Nat Rev Mol Cell Biol* **2**: 285–293

Zisch AH, Pazzagli C, Freeman AL, Schneller M, Hadman M, Smith JW, Ruoslahti E, Pasquale E (2000) Replacing two conserved tyrosines of the EphB2 receptor with glutamic acid prevents binding of SH2 domains without abrogating kinase activity and biological responses. *Oncogene* **19**: 177–187

©2005 European Molecular Biology Organization